EFFECT OF STRAIN-ACCELERATION ON PLASTIC DEFORMATION BEHAVIOUR OF ALUMINUM

A Thesis Submitted
in Partial Fulfillment of the Requirement
for the Degree of
MASTER OF TECHNOLOGY

by

KULKARNI SUBODH S.

to the

DEPARTMENT OF MECHANICAL ENGINEERING

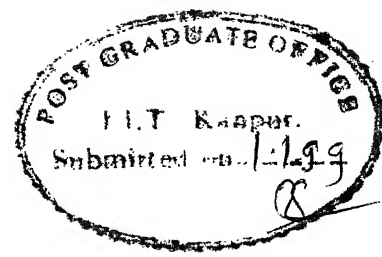*INDIAN INSTITUTE OF TECHNOLOGY - KANPUR*

JANUARY, 1999.

CERTIFICATE

It is certified that the work contained in the thesis entitled **"EFFECT OF STRAIN ACCELERATION ON PLASTIC DEFORMATION BEHAVIOUR OF ALUMINIUM"**, by Mr. **KULKARNI SUBODH.S,** has been carried out under our supervision and that this work has not been submitted elsewhere for a degree.

(Prof. V .K. JAIN)

Dept. of   Mech. Engg.
Indian Institute of Technology,
Kanpur 208 016, India

(Prof Om Prakash)

Dept. of   Mech. Engg.
Indian Institute of Technology,
Kanpur 208 016, India

JANUARY, 1999.

AKNOWLEDGMENTS

Dedicated to

THOSE WHO DON'T GET CHANCE OF FORMAL EDUCATION

AND TO THOSE WHO DON'T BELIEVE IN IT.

ABSTRACT

This work deals with strain-acceleration in plastic deformation behavior of aluminum.

Earlier studies have shown the significance of strain-acceleration in machining of metals. However, the phenomenon has never been investigated under simple loading conditions such as uni-axial tension and compression. Accordingly, this work was undertaken to study the effect of strain acceleration under uni-axial loading conditions and to attempt to investigate any co-relation it may have with strain acceleration under conditions encountered in metal cutting.

In metal cutting, the strain acceleration phenomenon occurs in machining operations like facing and taper turning where the cutting velocity changes continuously with time. Aluminum-specimens were studied under facing operations. Measurements of cutting force, temperature and chip parameters were performed to determine strain acceleration effect using a model proposed in an earlier work.

Uni-axial tension and compression tests were carried out on aluminum - specimen under displacement control to achieve a range of strain acceleration conditions, and the results analyzed using an appropriate model. A power law expression has been proposed to determine the dependence of flow stress on strain acceleration and strain hardening from this data.

Results on uni-axial tests and machining indicate that the flow stress is sensitive to 'strain acceleration'. Even though the strain acceleration values achievable under

two conditions differ by an order of magnitude, the strain hardening exponents and the strain acceleration-sensitivity derived for the two tests based on a power law expression proposed in this work are quite similar. This suggests that the constitutive equation proposed may be applicable more generally.

CONTENTS

List of Figure Captions

List of Tables

Nomenclature

A	Actual area (mm^2)
Ao	Initial area (mm^2)
b	Width of cut (mm)
d	Diameter of machining specimen (mm)
D_o	Inner diameter of machining specimen (mm)
D_A	Outer diameter of machining specimen (mm)
d	Diameter of tension and compression specimen (mm)
dl	Change in length (mm)
dt	Change in time (min)
ds	Thickness of Primary Shear Deformation Zone (mm)
F	Force applied ($kgf.$)
f	Feed (mm/rev)
k	Yield strain at $\varepsilon = 1$
L	Actual length of specimen (mm)
lo	Initial length of specimen (mm)
l	Strain acceleration sensitivity ($/mm^2$)
m	Modified strain hardening exponent
R, R'	Resultant force ($kgf.$)
r	Chip thickness ratio
t	Time (min)

V	Cutting velocity (m/sec)
Vc	Chip velocity (m/sec)
Vs	Shear velocity (m/scc)
α	Rake angle (°)
ε	Strain in uni-axial loading
$\dot{\varepsilon}$	Strain rate in uni-axial loading (/sec)
$\ddot{\varepsilon}$	Strain acceleration in uniaxial loading (/sec^2)
ε_t	True strain
γ	Shear strain
$\dot{\gamma}$	Shear strain rate (/sec)
$\ddot{\gamma}$	Shear strain acceleration (/sec^2)
$\ddot{\gamma}_f$	Shear strain acceleration in facing operation (/sec^2)
$\ddot{\gamma}_t$	Shear strain acceleration in taper turning (/sec^2)
λ	Friction angle (°)
σ_t	True stress (kgf/mm^2)
ϕ	Shear angle (°)
θ_t	Taper angle (°)

CHAPTER 1

INTRODUCTION

1.1 INTRODUCTION

Plastic deformation of metal at low strain rate is generally considered to be independent of rate of deformation. The plastic deformation is caused mainly by slip mechanism such as generation and movement of dislocations [1]. It is pertinent to express the deformation in terms of relation between stress (σ) and strain (ε) and can be expressed as,

$$\sigma = f(\varepsilon) \quad \text{..........................(1)}$$

In some metals like aluminium, copper and lead, the effect of strain-rate is quite pronounced specially at strain-rate above 100/sec. Yield stress increases with increasing strain rate and work hardening behavior is also found to be different.

It is generally believed that at higher strain-rate, it becomes difficult for dislocations to multiply and move. However it is still puzzling to find that some metals are not affected as far as the constitutive relation is concerned. That is why, materials are characterized as strain-rate sensitive and strain-rate insensitive. Therefore, in general, the flow stress is not only a function of strain but also dependent on strain-rate .i. e,

$$\sigma = f(\varepsilon, \dot{\varepsilon}) \quad \text{..(2)}$$

In machining operations, a thin strip of material is fractured out from the work-piece by the advancing tool tip and then it is sheared in the shear zone at a very high strain-rate.

When the material comes out of the shear zone, it is called a chip and its orientation is different from its original position so that it can conveniently slide over the

rake face of the tool. The strain rate within the shear zone varies with cutting speed and is constant for a given cutting speed. But in certain machining operations when cutting speed varies (for example, facing and taper turning), and hence the shear strain rate varies, this introduces a new variable *shear strain acceleration* [2]. The material response under such condition is in general different from that predicted by equation (2). Therefore, a more general constitutive equation may be proposed as:

$$\sigma = f(\varepsilon, \dot{\varepsilon}, \ddot{\varepsilon}) \dots\dots\dots\dots\dots\dots\dots\dots\dots(3)$$

An understanding of the functional form of the above equation is important from a practical viewpoint for predicting force and power requirement in processes such as machining and deformation processing. Equally important from a theoretical view –point, is a fundamental understanding of the nature of plastic deformation of materials subjected to such loading. The latter is studied more conveniently under simpler loading conditions such as uni-axial tension or compression.

The present work, therefore, aims to study the effect of strain acceleration on flow stress in machining as well as in uni-axial loading and draw comparisons in terms of material response.

1.2 CONSTITUTIVE LAW FOR PLASTIC DEFORMATION.

While considering the effect of loading variables on material response, it is convenient to consider the stress- strain response under uni-axial loading. The stress-strain curve obtained by uni-axial loading, as in an ordinary tension test, is of fundamental interest in plasticity when the curve is plotted in terms of true stress and true strain.

Typical true stress-true strain curve for a ductile metallic material is illustrated, Fig 1.1. [1]. Hooke's law is followed up to some yield stress. Beyond the yield stress the metal deforms plastically. Most metals strain-harden in this region, so that further increase in strain require higher values of stress than the initial yield stress, i.e. $\frac{d\sigma}{d\varepsilon}$ has a positive, non-zero value. However, unlike the situation in the elastic region, the stress and strain are not related by any simple constant of proportionality; instead we have an equation of the form, $\sigma = k\varepsilon^n$, where n is the strain hardening exponent (Table 1.1). If the metal is strained to point A (Fig.1.1), when the load is released the total strain will immediately decrease from ε_1 to ε_2 by an amount $\varepsilon_1 - \varepsilon_2$. The strain decrease $\varepsilon_1 - \varepsilon_2$ is the *recoverable elastic strain*. However, the strain remaining is not all permanent -plastic strain. Depending upon the metal and temperature, a small amount of the plastic strain $\varepsilon_1 - \varepsilon_2$ will disappear with time. This is known as *anelastic behavior*. Generally the *anelastic* strain is neglected in mathematical theories of plasticity.

A true stress-strain curve is frequently called a *flow curve* because it gives the stress required for the metal to flow plastically to any given strain.

SR.No.	' K ' psi	EXPONENT 'n'	CONDITION OF MATERIAL	MATERIAL
1	175000	0.05	H.C.P	TITANIUM
2	93000	.15	B.C.C	ANNEALED ALLOY STEEL
3	228000	.10	B.C.C	Q &T MED.C STEEL
4	105000	.13	B.C.C	MOLYBDENM
5	46000	.54	F.C.C	COPPER
6	130000	.50	F.C.C	Cu 30 % Zn
7	220000	.52	F.C.C	AUST.STAINLESS STEEL
8	77000	.26	ANNEALED	.05 % C STEEL
9	93000	.15	ANNEALED	S.A.E.4340 STEEL
10	228000	.10	QUENCHED AND TEMPERED 1000 ^{0}C	
11	178000	.19	QUENCHED AND ANNEALED 1000 ^{0}C	.6 % C STEEL
12	130000	.49	ANNEALED	70 / 30 BRASS
13	77100	.261	ANNEALED	.05 %C RIMMED STEEL
14	73100	.0234	ANNEALED AND TEMPER ROLLED	.05 % C KILLED STEEL
15	75500	.0234	ANNEALED IN WET H $_2$	.05 % C K DECARBURISED STEEL
16	93330	.156	ANEEALED	.05/.07 % PHOS.LOW C STEEL
17	169400	.118	ANNEALED	S.A.E. 4130 STEEL
18	154500	.156	ANNELED AND TEMPER ROLLED	S.A.E. 4130 STEEL
19	143000	.299	ANNEALED	TYPE 430 STAINLESS STEEL 17 % Cr
20	55900	.211	ANNEALED	ALCOA -24 S ALUMINIUM
21	48450	.211	ANNEALED	REYNOLDS R -301 ALUMINIUM

Table 1.1   Strain hardening exponents.

Many attempts have been made to fit mathematical equations to this curve. The most common is a power expression of the form,

$$\sigma_t = K\varepsilon_t^n \qquad \dots\dots\dots(4)$$

Where k is the stress at strain=1.0 and n is the strain hardening coefficient. This equation is valid only from the beginning of plastic flow to the maximum load at which the specimen begins to neck down. (i.e. the point where it begins to deform in an unstable manner.)

1.2.1 GEOMETRICAL INSTABILITY

The condition for initiating unstable flow after any amount of prior straining is that somewhere in the material, the next increment of strain-induced hardening be canceled out by an accompanying strain-induced softening [3]. Subsequently further straining will tend to concentrate in the location where resistance to continued flow is first lost.

The hardening may take many forms, but its effect is positive $\delta\sigma$ for the strain increment i.e. $\delta\varepsilon$ (Fig.1.2)[3]. Therefore, the rate (with respect to strain) of strain-induced hardening is $d\sigma/d\varepsilon$. This is also equivalent to the rate of increase of load-carrying ability per unit area. Letting the total ability of straining be $F = \sigma A$, the rate of increase per unit area is

$$\frac{1}{A}\frac{dF}{d\varepsilon} = \frac{d\sigma}{d\varepsilon} \qquad \dots\dots\dots(5)$$

The softening may be a result of geometrical changes, or of changes in the material, or both. In the ordinary tension test it is essentially all geometrical, coming from the area reduction, $-\delta A$, in the strain increment, $d\varepsilon = -\dfrac{\delta A}{A}$ (Fig.1.3).

With $F = \sigma A$ the rate of loss of load-carrying ability per unit area (the rate of strain-induced softening) is $(1/A)(dF/d\varepsilon)$, as it was for the hardening, but now dF is $-\sigma dA$ (instead of $+Ad\sigma$), so that necking is given by:

$$\frac{1}{A}\frac{dF}{d\varepsilon} = -\frac{\sigma dA}{Ad\varepsilon} = \sigma \qquad \dots\dots\dots\dots\dots\dots\dots\dots\dots\dots\dots(6)$$

1.2 .2 MATERAIL INSTABILITY

In special cases there can be no geometrical softening(instability). In uni-axial compression the area change is $+\delta A$, so that there is only geometrical hardening. In pure shear $\delta A = 0$, to rule out geometrical softening again. Yet instabilities in the form of localized flow on planes of more or less maximum shear can occur in both. This is because softening now has a materials origin.

Different softening possibilities are made apparent by recognizing that σ can be a function of many variables [3], like strain, strain rate, temperature, and even surface energy and pressure and, we will include "strain acceleration"; i.e.,

$$\sigma = f(\varepsilon,\dot{\varepsilon},\ddot{\varepsilon},T,\gamma,P).$$

Therefore the net rate of the materials-based strain-induced hardening is

$$\frac{d\sigma}{d\varepsilon} = \left(\frac{\partial\sigma}{\partial\varepsilon}\right) + \left(\frac{\partial\sigma}{\partial\dot{\varepsilon}}\right)\left(\frac{d\dot{\varepsilon}}{d\varepsilon}\right) + \left(\frac{\partial\sigma}{\partial\ddot{\varepsilon}}\right)\left(\frac{d\ddot{\varepsilon}}{d\varepsilon}\right) + \left(\frac{\partial\sigma}{\partial T}\right)\left(\frac{dT}{d\varepsilon}\right) + \left(\frac{\partial\sigma}{\partial\gamma}\right)\left(\frac{d\gamma}{d\varepsilon}\right) +$$
$$\left(\frac{\partial\sigma}{\partial P}\right)\left(\frac{dP}{d\varepsilon}\right) + \dots\dots\dots\dots\dots\dots\dots\dots\dots\dots\dots\dots\dots\dots\dots\dots \dots\dots(7)$$

Therefore, the stress at any point between yield and ultimate tensile strength may be interpreted in terms of the net effect of the various terms appearing in this equation. There is a competition between the various hardening

and softening processes and the actual magnitude of these processes determine the flow stress.

Temperature, pressure and surface energy are important as far as their effects on flow stress is concerned, but for the present work we are considering effects of strain, strain-rate and strain-acceleration

Although not the main focus of this work, the physical basis of the various terms in equation (7) is briefly described in the following section.

1.3 FACTORS AFFECTING FLOW STRESS

1.3.1 THE EFFECT OF STRAIN: STRAIN HARDENING

Strain hardening is caused by dislocations interacting with each other and with barriers, which impede their motion through the crystal lattice.

Many dislocations do not reach the surface of a crystal but interact elastically with other dislocations, and become anchored within the crystal forming a network. This is a progressive state of affair so the dislocation concentration gradually increases as the deformation proceeds, and the stress necessary to force a passage for the later dislocation is raised, causing strain hardening.

The empirical power law expression by Ludwik, $\sigma_t = k\varepsilon_t^n$ accounts for the strain hardening of the material, where ' n ' is strain hardening exponent and it indicates the degree of strain hardening. Some typical values of 'n' for different materials [4,5] are given in Table 1.1.

1.3.2- EFFECT OF STRAIN RATE.

As mentioned earlier, it becomes difficult for dislocations to multiply and move at high strain-rate leading to higher flow stress than at lower strain rate. Other effects have also been reported.

In body centered cubic metals, it has been observed that the frictional resistance to slip is increased at high strain-rate, (in the range 9.8E-6 to 80 in./in./sec.). McLean [6] has observed the general effect of straining at increasing strain rates on copper and tungsten and found that for copper strain hardening is intensified where as for tungsten strain hardening is not much affected by strain-rate in the temperature range chosen for these tests, i.e,-250 to +250 degree Celsius.

At still higher speeds, reaching to explosive loading, complications enter because plastic flow only occurs when propagating elastic wave arrives and the deformed shape is not always that which would be produced by a similar static load but depends on the shape of the wavefront [7]. A remarkable effect has been found to occur [8,9] when a metal is explosively loaded with very high pressures. Without the dimensions being changed significantly, the hardness can be raised to a level equivalent to severe strain hardening (For example, in such experiments an explosive load of 4200 kg/sq.mm. resulted in the hardness of annealed copper being raised from 54 to 132 units.) Metallographic examination showed that twin like markings were present in copper. An exceedingly high strain rate therefore produces a situation inside the metal that is different from

the ordinary one. This perhaps comes about because dislocations exhibit a relativistic effect whereby resistance to their movement rises without limit as their speed approaches a critical value near to that of sound in the metal. Consequently, beyond a certain point it is only possible to increase the strain rate by increasing the number of dislocations, and the ordinary forces due to stress field, intersection etc. are relatively unimportant compared with relativistic effect.

Adiabatic heating becomes significant at fast speed of 80in. /in./sec. appox. (About 8000%/sec). The effect is particularly marked beyond the UTS, because heating is then concentrated in small volume. In one experiment, the temperature rise in necked region was estimated to be 200 degree Celsius. Such a temperature rise softens the material and causes the load elongation curve to fall steeply. This effect is expected to set in at slower speeds at very low temperature, as well.

When the temperature is constant the test results generally fit well empirical constitutive equation of the form [10],

$$\sigma = k\varepsilon^n \dot{\varepsilon}^{n'} \quad \dots\dots\dots\dots\dots\dots\dots\dots\dots\dots\dots\dots\dots(8)$$

where k, n and n' depend on the operating temperature. The exponent n' is known as strain rate sensitivity, the common value of n' are in the range of 0.02 to 0.20. [3].

1.3.3 EFFECT OF TEMPERATURE

Test temperature has a significant effect on flow stress of metals. At high temperature enhanced plastic deformation can take place due to processes

relating to diffusion creep and thermally activated climb of dislocations leading to time dependent strain accumulation (creep)[6].

1.3.4 EFFECT OF PRESSURE

Tensile tests on ductile materials under superimposed hydrostatic pressure have revealed that the yield point and uniform elongation are unaffected by the applied pressure, but the strain to fracture increases with the intensity of the pressure [10].

1.3.5 EFFECT OF SURFACE ENERGY.

Surface energy depends too little upon strain for this to contribute to the level of flow stress in deformable solids [3].

The surface energy of the surfaces produced during the straining or during fracture is decisive in determining the fracture path (in particular, whether it is inter-granular or cleavage) and important in determining fracture stress [6]. The lower is the surface energy, lower need the applied stress to produce new surface.

1.3.6 EFFECT OF STRAIN ACCELERATION

Jain [2] has studied the effect of strain acceleration on tool-chip interface temperature, shear angle, tool-life equation and cutting forces in machinability tests.

The effect of strain acceleration is prominently seen during facing operation. Lowering of tool –chip interface temperature takes place at higher strain accelerations [Fig.1.4][2]. In other words, tool experiences harder material at higher strain acceleration.

Higher cutting speeds give rise to higher strain acceleration [2]. The shear angle ϕ is also found increased with cutting speeds, (Fig 1.5)[2]

The value of 'n' in the tool–life equation $VT^n = C$, is found increased at high strain acceleration [2]. This is in line with Fig.1.4, because at higher cutting speed (or at higher strain acceleration), the value of 1/n decreases hence tool-life also decreases.

The basic nature of cutting forces is found to be changed due to strain acceleration which is caused at higher cutting speeds as shown in Fig 1.6.[2]

Experimental work of Kumar [11], on torsion specimen reveals that the material yields at lower flow stress, at a certain strain-rate level if higher strain acceleration is used. The reason given is that, at a certain strain rate achieved through high strain acceleration, the dislocations interaction may not occur (due to lack of time), to the extent it would have been at that strain rate attained in normal way.

1.4 OBJECTIVE OF THIS THESIS

As described in the preceding section, there is considerable evidence that strain acceleration has an effect on flow stress. However, there has been no attempt to study the phenomenon under simpler loading conditions or to develop a constitutive law which accounts simultaneously for the effects of imposed strain rate and strain acceleration.

Accordingly, in this work we investigate this phenomenon under simpler loading conditions of uni-axial tension and compression, and propose a

constitutive equation to quantify the strain and strain acceleration sensitivity of flow stress in aluminium.

Similar information is also derived from machining tests on the same material in order to evaluate the applicability of constitutive law proposed.

As discussed in previous section, $\sigma = f(\varepsilon, \dot{\varepsilon}, \ddot{\varepsilon}, T, S, P........)$. In present work we are not varying parameters T, S, P and since time and variables depending on time can not simultaneously appear as independent variables and be treated as such in a constitutive relation, McCartney [13], we consider,

$$\sigma = f(\varepsilon, \ddot{\varepsilon}) \dots\dots\dots\dots\dots\dots\dots\dots\dots (9)$$

The exact form of Eq. (9) is not known, therefore, by analogy to equation (8) we propose a power law of the form,

$$\sigma = k\varepsilon^m \ddot{\varepsilon}^l \dots\dots\dots\dots\dots\dots\dots\dots\dots (10)$$

where, m is the strain-hardening exponent and l is the strain acceleration sensitivity of the flow stress.

1.5 THESIS OUTLINE

In chapter one, we have briefly looked at factors affecting flow stress of metals and have reviewed the role of strain acceleration in metal cutting. We have proposed an equation to account for the dependence of strain and strain-acceleration on the flow stress.

Following earlier studies, in chapter-2 we describe experimental study of strain acceleration in metal cutting and derive the various coefficients in the proposed equation.

Experimentation and related theory about strain acceleration in uni-axial loading test is discussed in chapter 3, along with the theoretical approach developed for the analysis of strain-acceleration effects.

Concluding remarks and scope for future work are given in chapter 4.

1.6 REFERENCES:

1. Dieter. G. E., "Mechanical Metallurgy", McGraw-Hill Kogakusha, Ltd., Second Edition, 1961.

2. Jain. V. K, "Strain Acceleration: A new concept in metal cutting and its effects on accelerated machinability tests", J. Engg. Prod. Vol.3. No.1, 1979, pp 15-26.

3. Backofen. W.A., "Deformation Processing", Addison Wesley, 1972.

4. Marin J., "Engineering Materials: their mechanical properties and applications", Prentice-Hall Series, 1952.

5. Askeland D. R., "The science and Engineering Materials." PWS-Kent Publications, 1989.

6. McLean D., "Mechanical Properties of Metals", John Wiley & Sons, 1962.

7. Rhinehart J. S.' "Behaviour of Metals under Impulsive Loads", A.S.M, 1954. Smith C. S. T.

8. Smith C. S., T.A.I.M.E., 1958,212, 574.

9. Appleton A. S., T.A.I.M.E., 1961, 221, 90.

10. Chakraborty J., "Theory of Plasticity", McGraw-Hill Book Co., 1987.

11. Verma S.K., 'Effect of strain acceleration on properties of aluminium." M.Tech Thesis, I.I.T, Kanpur. 1989.

12. Jain V.K., "Strain Acceleration and its application to accelerated machinability tests." J. Of the Institution of Engineers (I), vol. 64, pt ME 2, 1983.

13. McCartney L. N., "No time – gentleman please!" Philos. Mag., 33, 689, 95.
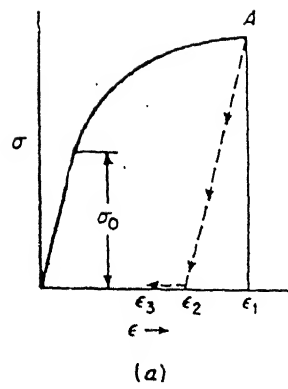
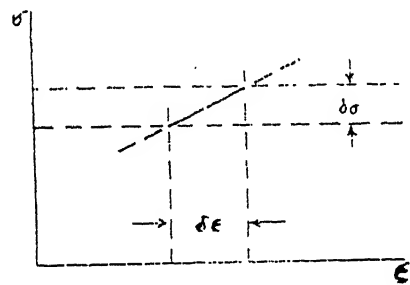Figure 1.1   Typical true stress-true strain curve for ductile metal.

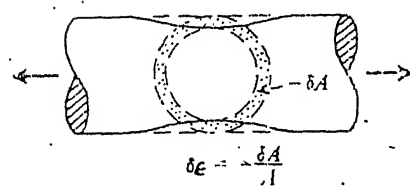Figure 1.2   Strain-induced hardening.

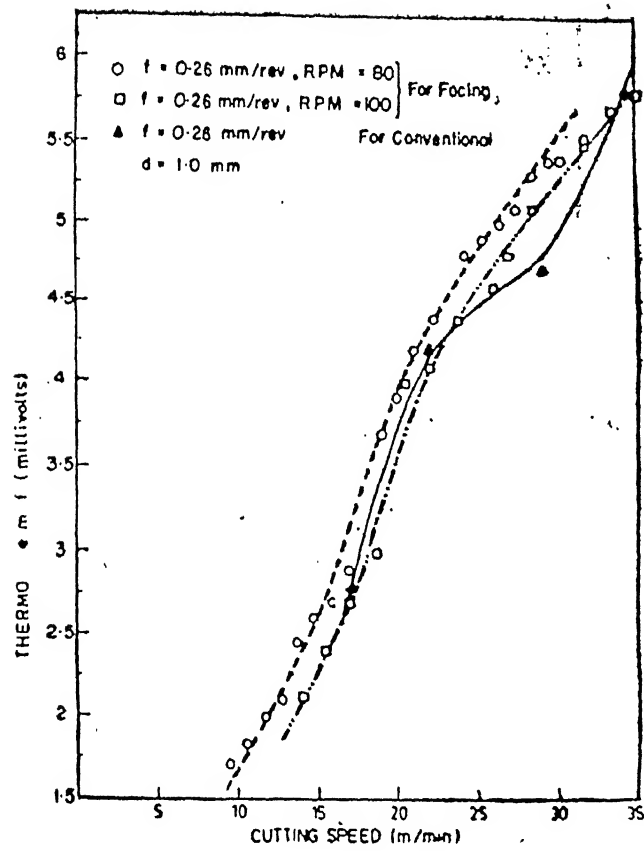Figure 1.3   Geometrical softening in an incipient neck.

Figure 1.4　Variation of thermo-e.m.f with speed in metal cutting. [2]
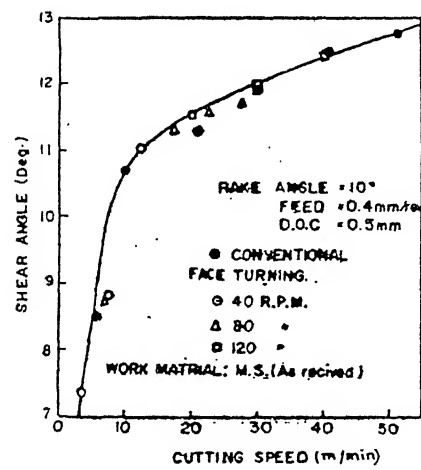

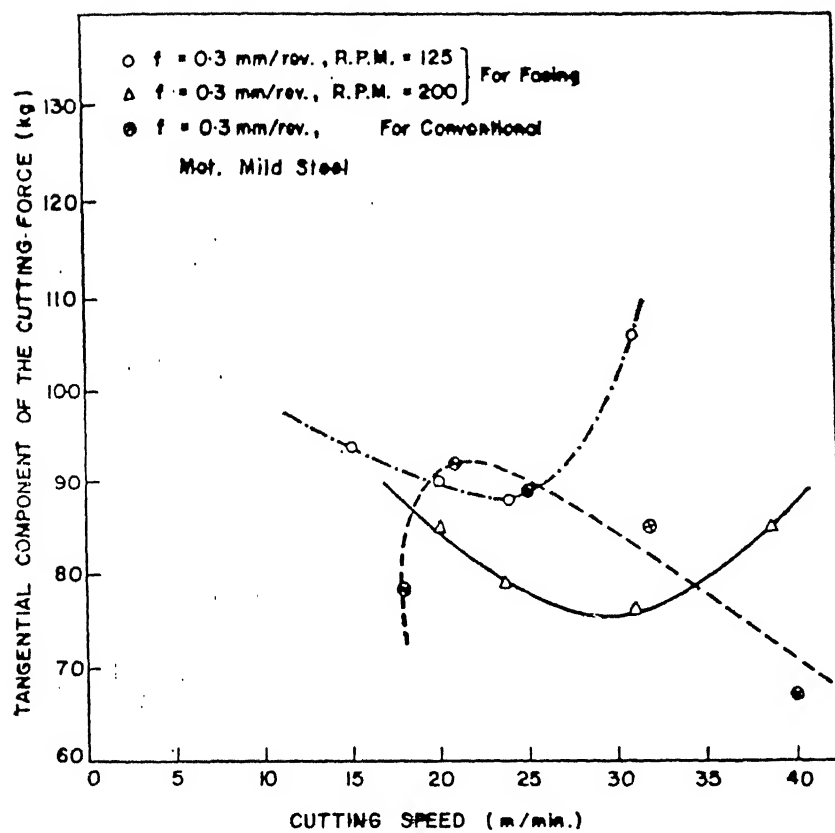Figure 1.5　Variation of shear angle with speed in metal cutting. [2]

Figure 1.6   Variation of cutting force component with speed in metal cutting. [2]

CHAPTER – 2

STRAIN ACCELERATION IN METAL CUTTING

2.1 - INTRODUCTION

Basically all single-point machining operations can be considered as either oblique or orthogonal cutting operations, former requiring three dimensions to specify and the latter two. Since most practical cutting operations are complex, the simple case of orthogonal cutting where a straight edge tool moves relative to the work-piece, in a direction perpendicular to its cutting edge has received maximum attention.

Fig.2.1 (a) shows the idealized model of continuous chip formation during orthogonal cutting. Various forces appear due to the interaction between the tool and work-piece, and are conventionally represented as a complete force diagram Fig 2.1 (b).[1] In drawing this force equilibrium diagram, the simplifying assumptions that have been made are:

1. The tool tip is sharp (zero edge radius) and the chip makes contact only with the rake face of the tool.

2. The cutting edge is perpendicular to the chip velocity.

3. The deformation is two - dimensional, i.e. no side spread.

4. The deformation takes place in a very thin zone so that a plane (AB), called the shear plane could reasonably represent the deformation zone.

5. Continuous chips without built – up – edge (B.U.E) are formed.

6. The work-piece material is rigid, perfectly plastic.

7. The coefficient of friction is constant along the chip-tool interface.

8. The resultant force on the chip R' applied at the shear plane is equal, opposite and collinear to the resultant force R applied to the chip at the chip-tool interface.

The material in the shear zone undergoes a large amount of plastic deformation prior to fracture, which leads to chip deformation.

Schematic diagram showing the interaction between a single-point-cutting tool and the work-piece is shown in Fig.2.1(a).

The shear strain γ is defined as $\dfrac{\Delta s}{\Delta y}$ with respect to a unit element, as shown in Fig.2.2.[1] In metal cutting (Fig 2.3), the deformation is idealized as a process of block slip of preferred slip planes as shown in Fig. 2.4.[1]

The resulting shear strain can therefore be represented as,

$$\gamma = \frac{\Delta s}{\Delta y} = \frac{AB'}{C'D'} = \frac{AD'}{CD'} + \frac{D'B'}{C'D'} \quad \dots\dots\dots\dots\dots(1)$$

The rate at which the shear strain γ is produced is given by,

$$\dot{\gamma} = \frac{\Delta s}{\Delta y} \cdot \frac{1}{\Delta t} \quad \dots\dots\dots\dots\dots\dots\dots\dots\dots\dots(2)$$

Where, Δt is the time required for the metal to travel the distance Δs along the shear plane. Δy as before is the distance between two successive shear planes. γ can also be expressed in terms of shear velocity, which can be obtained from the velocity diagram[1]. Fig.2.5 gives the following velocity relation-ships:

$$Vc = \frac{\sin\phi.}{\cos(\phi-\alpha)}.V \; ; \quad Vs = \frac{\cos\alpha}{\cos(\phi-\alpha)}.V \quad \dots\dots\dots\dots\dots(3)$$

Where, Vc, V, and Vs are chip velocity, cutting velocity and shear velocity respectively.

Hence,

$$\dot{\gamma} = \left(\frac{\Delta s}{\Delta t}\right).\frac{1}{\Delta y} = \frac{Vs}{\Delta y} \quad \dots\dots\dots\dots\dots\dots\dots\dots(4)$$

Or $\dot{\gamma} = \dfrac{\cos\alpha}{\cos(\phi-\alpha)} \cdot \dfrac{V}{\Delta y}$

In case of longitudinal turning operation under orthogonal cutting conditions at constant cutting speed, using orthogonal cuts, the strain rate ($\dot{\gamma}$) calculated using equation,

$$\dot{\gamma} = \dfrac{\cos\alpha}{\cos(\phi-\alpha)} \cdot \dfrac{V}{\Delta y} \quad\quad\quad\quad\quad\quad\quad\quad(5)$$

While machining at constant cutting speed, the strain rate as given by equation (5) is practically constant. However, in facing and taper turning (Fig.2.6),

continuous cutting speed variation results into change in the values of Δy and ϕ with time and hence at any instant of time t, strain rate ($\dot{\gamma}_f$) for facing [2] would be equal to,

$$\dot{\gamma}_f = \dfrac{\Pi N}{1000}(D_0 + 2Nft)\dfrac{\cos\alpha}{\Delta y\cos(\phi-\alpha)} \quad\quad\quad\quad[6(a)]$$

For taper turning,

$$\dot{\gamma}_t = \dfrac{\Pi N}{1000}\left[D_A + (D_A - D_B)\dfrac{Nft}{L}\right]\dfrac{\cos\alpha}{\Delta y\cos(\phi-\alpha)} \quad\quad\quad\quad[6(b)]$$

The distance Δy is a re-presentative distance of a single block and is called as the "primary shear deformation zone" (PSDZ) and is also denoted is by ds henceforth.

Some idea of the extent of the exponent of variation in ϕ and d_s with cutting speed may be obtained from the published data[3] for the case of longitudinal turning of steel. The changes in ϕ and d_s are small even for a large change in V. To simplify the analysis; changes in ϕ and d_s with cutting speed changes can be assumed to be insignificant.

It has been reported [3] that during orthogonal cutting of steel using H.S.S cutting tools, cutting speed variation between 0.097 m/s (9 ft/m) and 2.59 m/s (510 ft/m) resulted in

variations in *ds* from 0.021 to 0.017 cm (19 % reduction) and the corresponding variation in ϕ was from, 26^0 to 27.8^0, (6.9 % increase) respectively. Thus as an approximation, the effect of cutting speed variation on ϕ and *ds* can be neglected.

The value of d_s (i. e. mean width of PSDZ) in the above equations can be determined [4], from the equation (7) by performing simple experiments to determine ϕ rather than conducting cumbersome experiments using quick stop devices to actually measure d_s under microscope. The value of d_s is given by the equation,

$$d_x = \frac{\sqrt{2}}{4} \left(\frac{t_1 \sin\left(\frac{\pi}{2} + \alpha - \phi\right)}{\sin\phi \sin\left(\frac{\pi}{4} - \alpha + \phi\right)} \right) \quad\dots\dots\dots\dots\dots\dots\dots(7)$$

Therefore, from equation (5), rate of change of strain rate i.e., strain acceleration during facing and taper turning can be obtained for facing as,

$$\ddot{\gamma}_f = \frac{2\pi fN^2}{1000} \frac{\cos\alpha}{d_s \cos(\phi - \alpha)} \quad\dots\dots\dots\dots\dots\dots\dots\dots\dots\dots\dots [8(a)]$$

and for taper turning as,

$$\ddot{\gamma}_t = \frac{2\pi fN^2}{1000} \frac{\tan\theta_t \cos\alpha}{d_s \cos(\phi - \alpha)} \quad\dots\dots\dots\dots\dots\dots\dots\dots\dots[8(b)]$$

From equations [8(a), 8(b)], it can be seen that $\ddot{\gamma}$ in face turning and taper turning is proportional to square of the spindle speed employed.

2.2 Experimental Details

Orthogonal-Facing tests were conducted on aluminum to find out shear-strain-acceleration effects on plastic deformation during the machining process.

The cutting velocity during facing operation decreases if the cut is carried out from outer periphery towards center and increases if reversed. Experiments were conducted without coolant on commercially available aluminum round bars of 16-mm. dia. Experiments were also conducted using coolant for 16-mm aluminum bar. Precautions were taken in selecting the material from the same charge as for the uni-axial loading test (discussed in the following chapter).

Experiments were planned according to the design of experiments to reduce the total number of experiments and to get the data uniformly from all regions of selected working area. The design of experiments called 'central composite rotatable design' [5] for two factors was adopted as; this design is normally used in the following conditions when,

1. No linear relationship between the input and output variables exists.

2. More than two levels are required for each of the input variables.

3. Repeatability of the experiments required is quite good.

These conditions are largely satisfied in the present case; hence the central composite rotatable design has been adopted.

All the experiments were carried out at room temperature on HMT, LB-25 type lathe machine.

Fig.2.7 shows the schematic diagram of the experimental set-up. Orthogonal facing operations were conducted at various spindle speeds and feed values, details of which are given in 'plan of experiments'.

2.2.1 Plan of Experiments

Experiments conducted were planned using statistical techniques so that useful inferences could be obtained by performing minimum number of experiments. The general

form of a quadratic (second-degree) polynomial equation is illustrated by the following equation [9].

$$y_u = b_0 + \sum_{i=1}^{k} b_i \, x_{iu} + \sum_{i=1}^{k} b_i \, x_{iu}^2 + \sum_{i<j}^{k} b_{ij} \, x_{iu} \, x_{ju} \qquad \dots\dots\dots\dots\dots\dots(9)$$

where, x_{iu} represents the levels of the ith factor in the uth experiment,

x_{iu}, x_{ju} = Variables., y_u = Response at the uth observation.

k = no. of variables.

b_i = Regression constants

The design for two x - variables is shown in Table 2.1.

Table 2.1 Central composite rotatable design for k=2

Sr.N.	X_0	X_1	X_2	X_1^2	X_2^2	$X_1 X_2$
1	1	-1	-1	1	1	1
2	1	1	-1	1	1	-1
3	1	-1	1	1	1	-1
4	1	1	1	1	1	1
5	1	-1.414	0	2	0	0
6	1	1.414	0 .	2	0	0
7	1	0	-1.414	0	2	0
8	1	0	1.414	0	2	0
9	1	0	0	0	0	0
10	1	0	0 ·	0	0	0
11	1	0	0	0	0	0
12	1	0	0	0	0	0
13	1	0	0	0	0	0

Subsequent steps are as follows:

1. Complete the columns headed $x_0, x_1, x_2, x_1^2, x_2^2, x_1 x_2$ as shown. The two-way array with 6 columns and 13 rows comprises the X - matrix of the x-variables. The corresponding values of the response Y are placed on the right.

2. Form the sum of products of each column in the matrix X with the column of Y values. These sums of products are denoted by (0y), (1y), (2y) and so on.

3. From the values of (0y), (1y), etc. the regression coefficients* are computed directly from the equations given below [12].

$$b_0 = 0.2(0y) - 0.1\sum iiy$$

$$\sum iiy = (11y) + (22y)$$

$$b_i = 0.125(iy)$$

$$b_{ii} = 0.125(iiy) + 0.01875\sum(iiy) - 0.1(0y)$$

$$b_{ij} = 0.25(ijy)$$

.........................(10)

In the present analysis of the experiments, the effect of strain-acceleration on plastic deformation was studied with varying parameters, viz. feed (f) and rpm (N). A preliminary step is to set up the relations between the coded x - scales and the original scales in which the levels are recorded. In design scale, the lowest and highest values of x are -1.414 and 1.414.

Ranges of feed and spindle speed are taken as:

$$F = 0.03 - 0.1 \text{ mm./rev}$$

$$N = 40 --- 320 \text{ rpm}$$

$$x = -1.414 \text{ when } f = 0.03 \text{ mm./rev., } N = 40 \text{ RPM}$$

$$x = 1.414 \text{ when } f = 0.1 \text{ mm./rev., } N = 320$$

Then, in general,

$$x = a + b * \text{(variable)}$$

'a' and 'b' are chosen to satisfy the desired conditions at the ends of the scale.

(i) Feed (f):

$$x = a + b * (f)$$

when $x = -1.414$; f = 0.03 mm./rev and so, $-1.414 = a + b * 0.03$

when $x = 1.414$; f = 0.1 mm./rev and so, $1.414 = a + b * 0.1$

On solving these two equations simultaneously we get,

a = -2.626

b = 40.4

So,

x= -2.626 + 40.4 * f ....(11)

Similarly for temperature

x= -2.626 +40.4 * N ....(12)

From (11) and (12), feed and spindle speed corresponding to level x = -1, 0, 1 are determined. The complete conversion is tabulated in Table 2.2.

Table 2.2 Conversion Table

X	Feed(f)	Spindle speed(N)
-1.414	0.03	40
-1	80	0.042
0	200	0.066
1	250	0.083
1.414	320	0.10

With the above conversions, the experiments are conducted in random order according to the plan given in the Table 2.3

Table 2.3: Plan of Experiments.

Exp. No.	S.No. Acc. to design of exp. (Table 3.1)	Feed(X_1) (mm./rev)	Spindle speed (X_2) (rpm)
1	5	0.042	80
2	1	0.066	40
3	11	0.066	250
4	3	0.066	200
5	13	0.066	200
6	8	0.1	200
7	2	0.042	250
8	4	0.083	250
9	7	0.03	200
10	6	0.066	320
11	9	0.066	200
12	10	0.066	200
13	12	0.066	200

NOTE: ALL THE ABOVE VALUES ARE THE NEAREST VALUES OF FEED AND

SPINDLE SPEED AVAILABLE AT MACHINE, TO THAT OF OBTAINED BY DESIGN OF

EXPERIMENTS.

2.3 RESULTS AND DISCUSSION

Experimental observations involved recording of entities, viz. cutting force and feed force with the help of turning dynamometer, and measurements of deformed chip-thickness. Calibration of voltage vs. forces was carried out as the recorder output for the forces is in mili-volts (Fig.2.8). Records of forces have been plotted on graph-sheet with x-y plotter (Fig.2.9). Chip thickness was measured directly with the help of micrometer. Chip thickness measurements in turn give the chip-thickness ratio, which is a ratio of uncut chip thickness or feed and deformed chip thickness. The chip thickness ratio is used to calculate shear angle. Cutting force and feed force are considered for evaluating shear stresses.

The details of experiments and corresponding results are given in Table2.4 and Table-2.5.

2.3.1 Outline of Formulae Used.

The theoretical approach developed [2] to achieve the shear strain acceleration after conducting experiments and recording the necessary parameters is as follows.

Quantities feed, spindle speed, cutting force and feed forces are known, deformed chip is measured. Using these basic quantities chip-thickness ratio, shear angle, mean thickness of primary shear deformation zone, strain, strain rate and strain acceleration can be found out. Following are the formulae [3,4] used,

1. Chip-thickness- ratio α) $= \dfrac{t_1}{t_2} = \dfrac{f}{t_2}$

$$\begin{bmatrix} \because t_1 = f \\ as \rightarrow t_1 = f \cos\gamma_s \\ and - \gamma_s = 0 \\ t_1 = f \end{bmatrix}$$

2. Shear angle $(\phi) = \tan^{-1}\left[\dfrac{r\cos\alpha}{1-r\sin\alpha}\right]$ $\qquad\left[\alpha = 0^{0}\right]$

3 Thickness of Primary Shear Deformation Zone (d_s)

$$d_s = \frac{\sqrt{2}}{4}\left(\frac{t_1\sin\left(\dfrac{\pi}{2}+\alpha-\phi\right)}{\sin\phi\sin\left(\dfrac{\pi}{4}-\alpha+\phi\right)}\right)$$

4. Strain, $(\gamma) = \tan(\phi-\alpha)+\cot\phi$

5. Strain Rate $(\dot{\gamma}) = \dfrac{\pi N(D_0 + 2\pi ft)\cos\alpha}{1000d_s\cos(\phi-\alpha)}$ and $\left[t = \dfrac{l}{f.N}\right]$

6. Strain Acceleration $(\ddot{\gamma}) = \dfrac{2\pi f N^2\cos\alpha}{1000d_s\cos(\phi-\alpha)}$

7.Shear Stress $(\sigma_s) = \dfrac{(f_s\cos\phi - f_f\sin\phi)\sin\phi}{b.t}$

SR. No.	FEED f[mm/rev]	SPEED N[rpm]	DEPTH OF CUT d[mm]	CHIP THK. RATIO r	SHEAR ANGLE φ[deg]	THK.OF PSDZ ds[μm]	CUTTING FORCE Fc[kgf]	FEED FORCE Ff[kgf]	SHEAR STRESS σs'[MPa]	S. STRAIN RATE $\dot{\gamma}$ [/sec]	S. STRAIN ACCELN $\ddot{\gamma}$ [/sq.sec]	SHEAR STRAIN γ
1	0.042	80	1.00	0.200	11.31	89	7.00	5.75	267.8	0.76	0.0053	5.20
2	0.042	250	1.00	0.126	7.18	149	8.00	6.25	212.6	1.41	0.0308	8.07
3	0.083	80	1.00	0.263	14.72	129	11.80	8.00	287.1	0.53	0.0074	4.06
4	0.083	250	1.00	0.358	19.68	90	9.00	8.00	234.5	2.45	0.1060	3.15
5	0.066	40	1.00	0.214	12.06	130	10.00	7.00	263.2	0.26	0.0014	4.89
6	0.066	320	1.00	0.236	13.26	116	10.00	7.00	282.5	2.37	0.1041	4.47
7	0.100	200	1.00	0.258	14.49	158	13.50	8.50	273.8	1.10	0.0454	4.12
8	0.066	200	1.00	0.253	14.19	107	10.00	8.00	287.3	1.61	0.0442	4.20
9	0.066	200	1.00	0.254	14.24	106	9.50	7.00	279.0	1.62	0.0444	4.19
10	0.066	200	1.00	0.208	11.80	133	10.60	7.50	273.9	1.28	0.0352	4.99
11	0.066	200	1.00	0.275	15.38	97	9.00	6.25	282.1	1.78	0.0489	3.91
12	0.066	200	1.00	0.255	14.35	106	9.50	7.00	280.5	1.63	0.0448	4.16
13	0.066	200	1.00	0.245	13.69	112	9.000	7.000	254.2	1.54	0.0428	4.34

Table 2.4 Results of experiments; Dia.of Aluminium bar 16-mm. ,without coolant.

SR NO	FEED f[mm/rev]	SPEED N[rpm]	DEPTH OF CUT d[mm]	CHIP THK. RATIO r	SHEAR ANGLE φ[deg]	THK.OF PSDZ ds[μm]	CUTTING FORCE Fc[kgf]	FEED FORCE Ff[kgf]	SHEAR STRESS σs [MPa]	SHEAR STRAIN γ	S. STRAIN RATE $\dot{\gamma}$ [/sec]	S. STRAIN ACCELN $\ddot{\gamma}$ [/sq.sec]
1	0.042	80	1.00	0.280	15.64	61	7.20	4.60	365	3.85	1.14	0.0080
2	0.042	250	1.00	0.155	8.84	118	7.00	4.60	227	6.58	1.79	0.0392
3	0.083	80	1.00	0.437	23.60	72	9.00	5.00	301	2.72	1.01	0.0140
4	0.083	250	1.00	0.553	28.96	55	9.50	5.50	329	2.36	4.33	0.1875
5	0.066	40	1.00	0.330	18.26	79	8.00	5.50	279	3.36	0.44	0.0024
6	0.066	320	1.00	0.413	22.42	61	8.00	5.75	301	2.84	4.73	0.2082
7	0.100	200	1.00	0.666	33.69	54	11.20	4.25	386	2.17	3.72	0.1551
8	0.066	200	1.00	0.507	26.92	48	8.00	5.00	334	2.48	3.88	0.1068

Table 2.5 Results of experiments; Dia.of Aluminium bar 16-mm. ,with coolant.

2.3.2 FEED, CUTTING-SPEED AND STRAIN-ACCELERATION.

It has been found theoretically that strain acceleration is directly proportional to square of the spindle speed employed and directly proportional to feed.

Fig.2.10 shows the relationship between feed and strain acceleration; when feed is considered individually, low feed rate result in low strain acceleration. At feed rate as low as 0.042 mm./rev., the magnitude of strain acceleration is insignificant about 0.02 /sq.sec., but at higher feed rate (0.1 mm./rev), the strain acceleration value is 0.1/sq.sec i.e. the value of strain acceleration has increased five fold.

Fig.2.11 illustrates effect of spindle speed on strain acceleration. Spindle speed is found to be critical factor affecting strain acceleration during facing operation. At low spindle speeds the strain acceleration is limited to a value 0.04/sq.sec., but at higher spindle speeds say beyond 200 rpm the strain acceleration value attained is as high as 0.1 /sq.sec.

2.3.3 SHEAR STRESS, SHEAR STRAIN AND STRAIN-ACCELERATION.

Fig.2.12, illustrates the relationship between shear stress, shear strain and strain acceleration.

It is found that shear stress increases from 50 MPa. to 150 MPa. as the strains are increased. The shear stresses remain approximately constant in the range 250-300 MPa., even at considerable increase in strain value beyond 3.

The strain hardening exponent (m) and the strain acceleration sensitivity of flow stress (l) as per the constitutive equation proposed ($\sigma = k.\varepsilon^{m}.\ddot{\varepsilon}^{l}$) in chapter-1 were obtained by Linear-multiple-regression analysis (outlined in Appendix A) of the above data.

The values are m = 0.230 and I = 0.017,and k = 35.49 (kg/sq.mm), and the constitutive equation is,

$$\sigma_s = 35.49\gamma^{0.230}\dot{\gamma}^{0.017}.$$

The strain-hardening exponent is in good agreement with literature values (Table 1.1)

2.4 REFERENCES:

1. Lal G.K., " Introduction to Manufacturing Science", New Age International Ltd. Publishers, 1996.

2. Jain. V.K., "Effects of strain acceleration in machinability tests." proceedings of the 8th AIMTDR Conference, I.I.T, Bombay, 1978.

3. Stevenson M.G. and Oxley P.L., "An experimental Investigation of the influence of speed and strain rate on the strain rate in a zone of intense plastic deformation". Proc. of The institution of mechanical engineers (Applied Mechanics), vol. 184, no 31,1969, p 561.

4. Jain V.K, Bandyopadhyay D.K, "Shear Angle during Accelerated Cutting: Response Surface Analysis." Int. J. M.T.D.R., Vol. 26, no. 1, pp. 35-50, 1986.

5. Cochran W. G and Cox G. M, " Experimental Designs", Asia Publishing House, New Delhi, 1962.
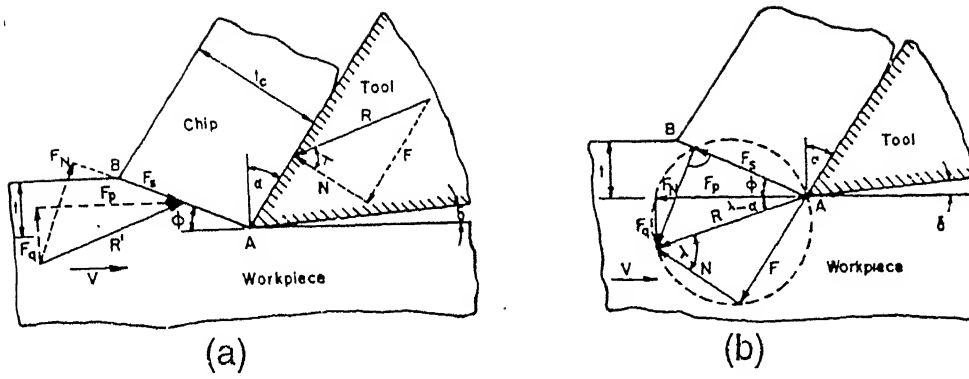
Figure 2.1   Force diagram in single-point cutting operation.

$$\gamma = \frac{\Delta s}{\Delta y}$$
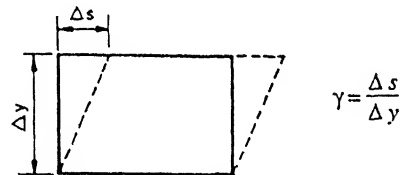
Figure 2.2   Definition of shear strain.
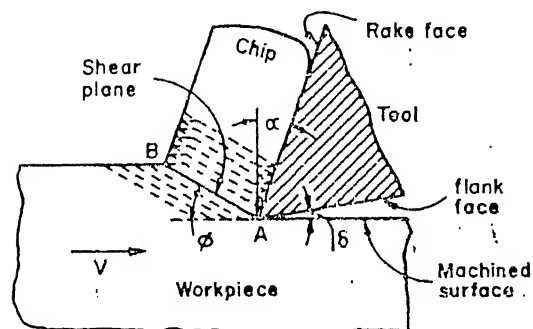
Figure 2.3   Definition of various terms in single-point cutting operation.
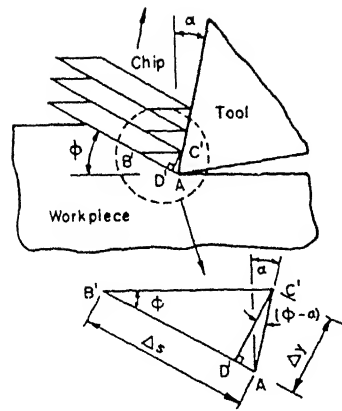
Figure 2.4 Visualization of preferred plane concept in single-point cutting operation.
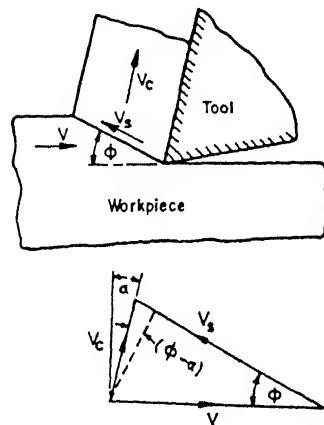
Figure 2.5 Velocity Diagram for single-point cutting operation.

TAPER - TURNING

FACING

1 HOT JUNCTION
2 COLD JUNCTION
3 WORKPIECE
4 INSULATION
5 Hg CONTACT
6 THERMOCOUPLE AMPLIFIER
7 DYNAMOMETER
8 BRIDGE AND AMPLIFIER

(a)

(b)

(c)
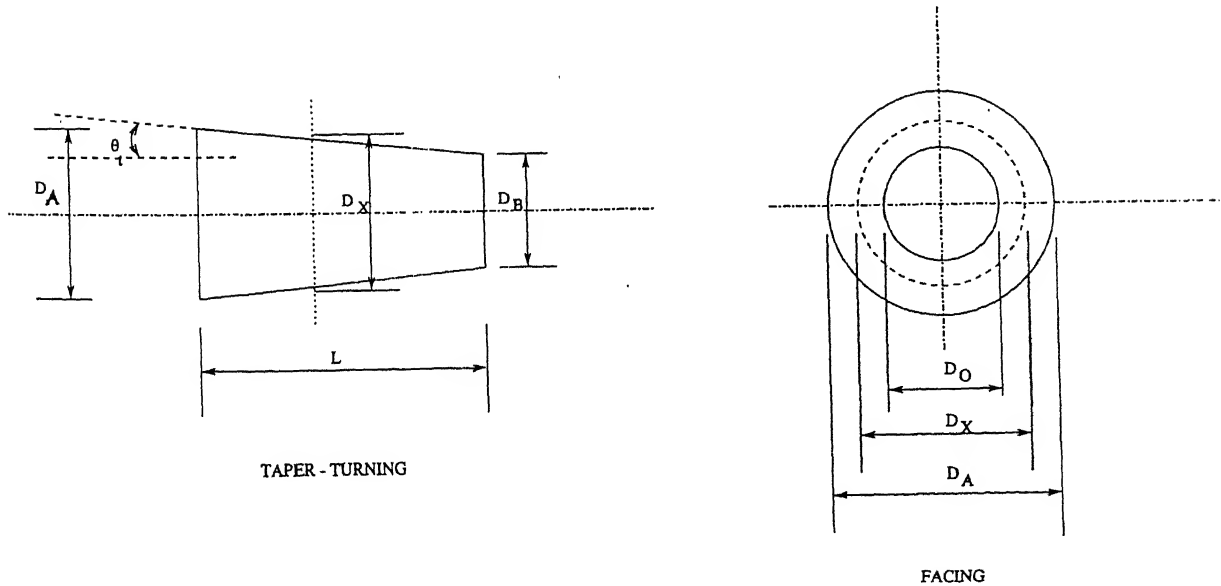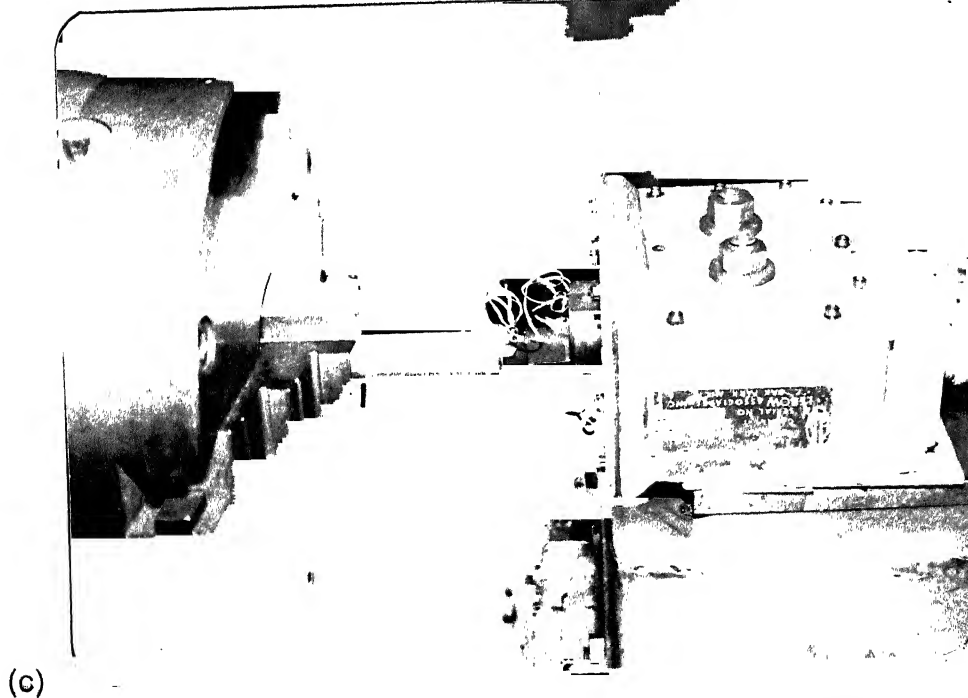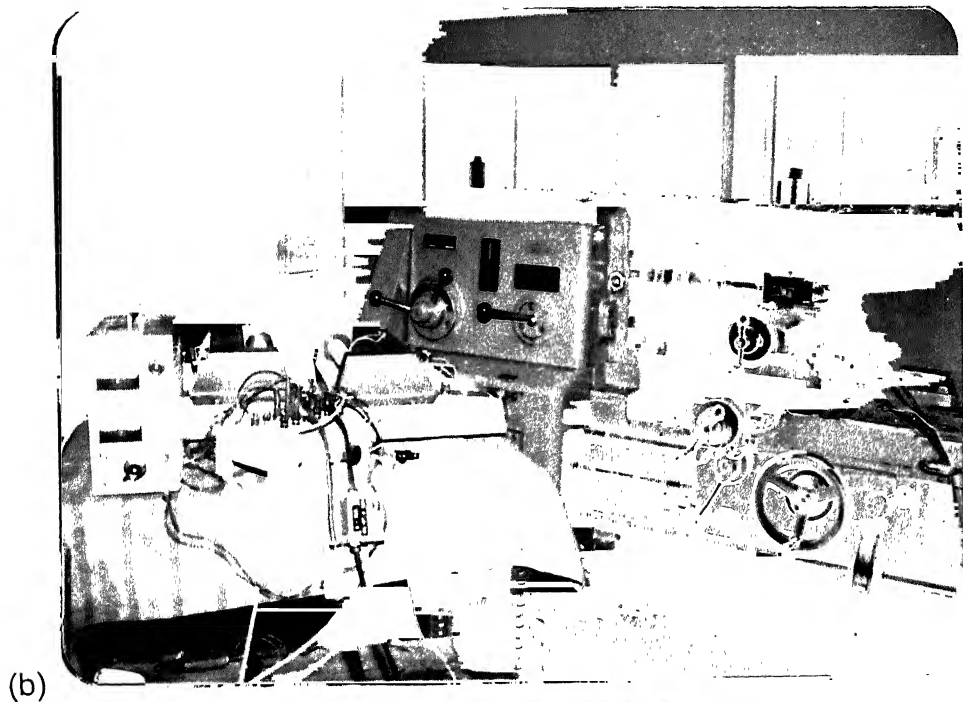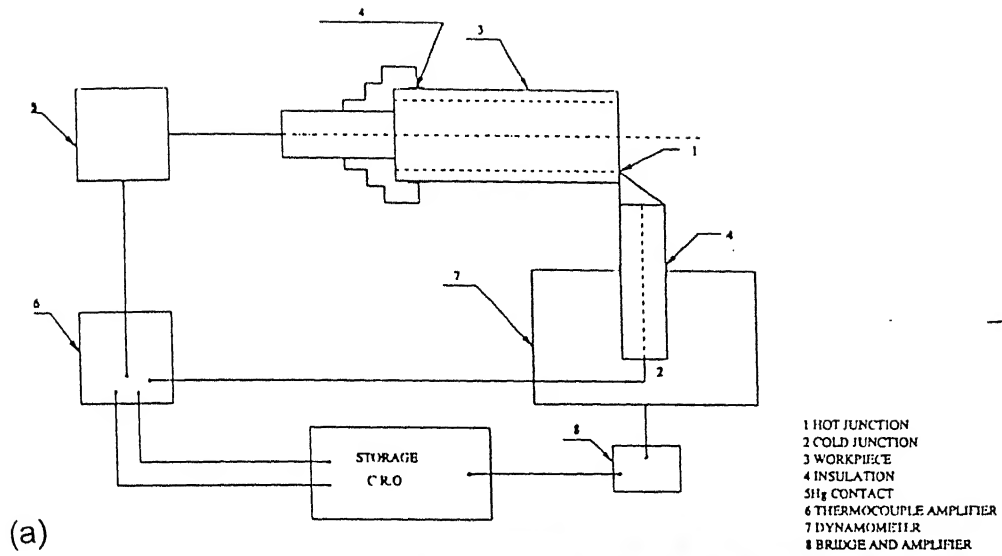
Figure 2.7   Experimental set-up for machining tests: (a) Schematic diagram (b) photograph of the set-up, and (c) Magnified view close to the cutting point
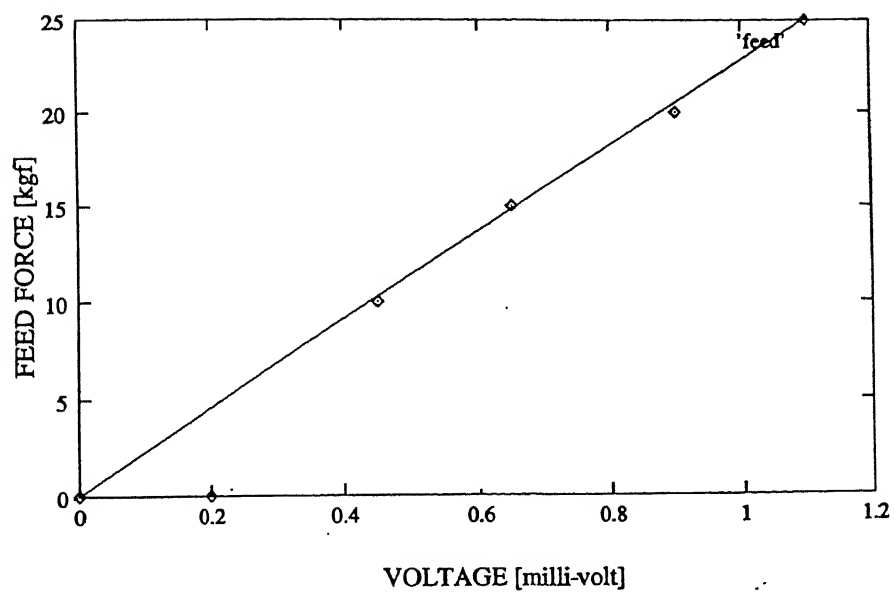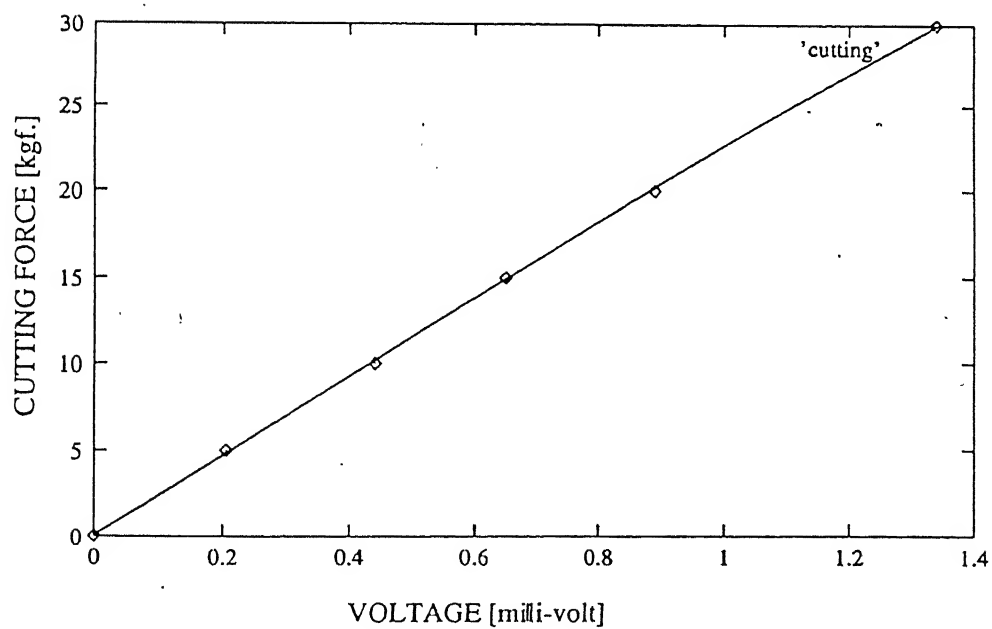
Figure 2.8   Calibration-curves showing (a) Feed force versus voltage output and (b) Cutting force versus voltage output.
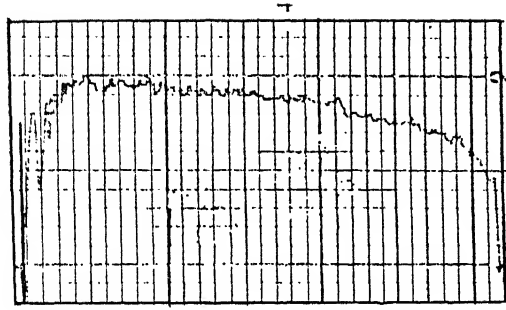
FOR   CUTTING FORCE

Scale 1 div =0·05 mV.
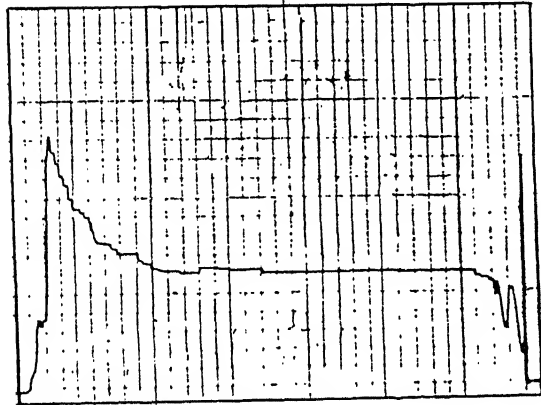
FOR FEED FORCE

Figure 2.9   Typical record of forces from the experiments.

[Sr. No. 5, Table 2.4]
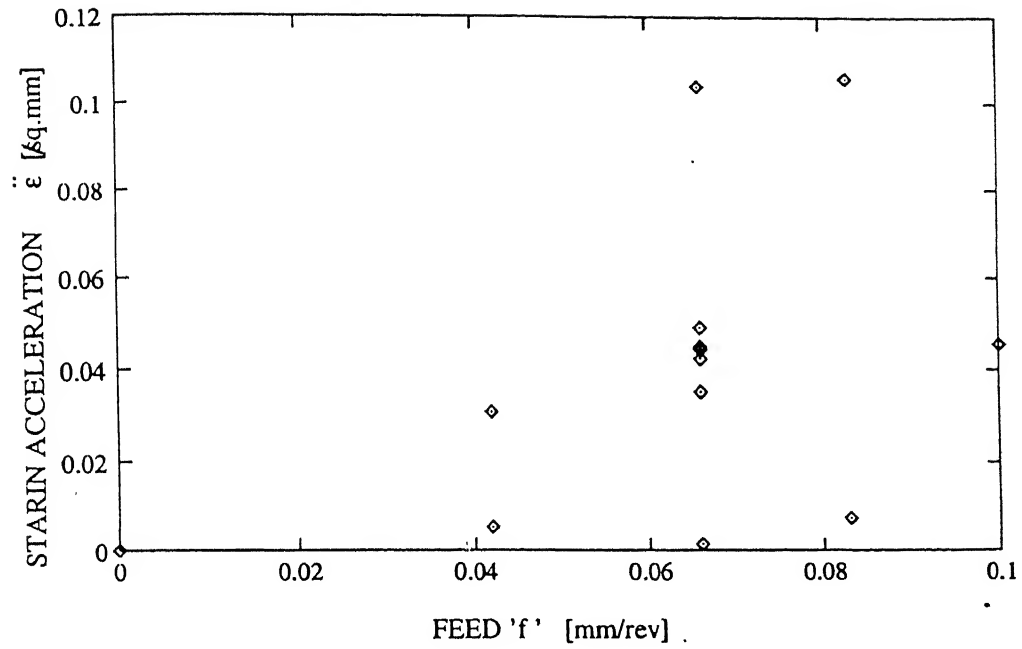
Figure 2.10   Variation of shear-strain acceleration with feed in facing of aluminium.
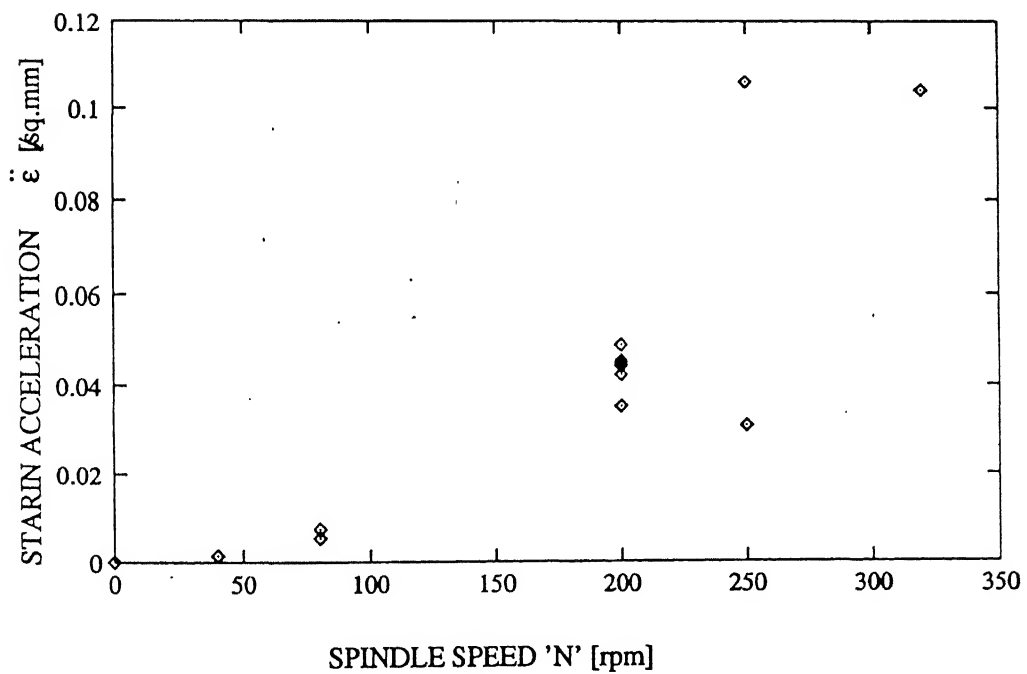
Figure 2.11   Variation of shear-strain acceleration with
spindle speed in facing of aluminium.
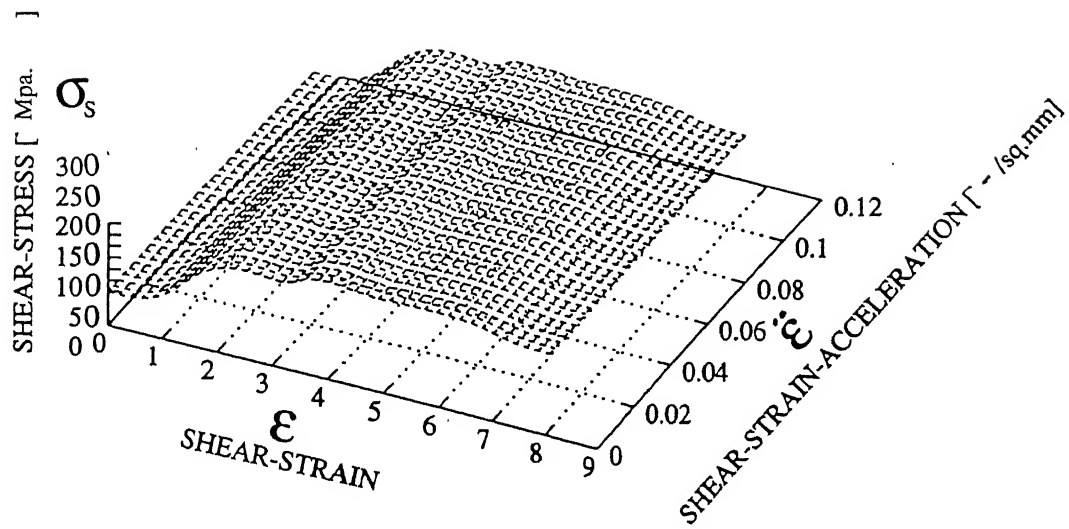
Figure 2.12   Diagram showing the variation of shear stress with
shear strain and shear strain-acceleration.

CHAPTER - 3

STRAIN ACCLERATION IN UNI-AXIAL LOADING.

3.1 - INTRODUCTION

In constant strain rate test, the specimen is held between the grips or platen in a mechanical testing machine and extended or compressed as the cross head is driven up or down at constant speed.

The force exerted is measured by a load cell and recorded as a function of time. The length of the sample varies linearly with time hence strain rate relative to initial length is constant but the actual strain rate is not.

Although it is commonly used, the name 'constant strain rate test ' is misleading [1]. The true strain rate can be considered constant only at small strains. The force-time curve is usually transformed to a true stress-strain curve. The true strain is obtained using expression,

$$\varepsilon_t = \ln\left[\frac{1 \pm \Delta l(t)}{l_0}\right] \quad \dots\dots\dots(1)$$

and the true stress is obtained by dividing the applied load or force F, by the current cross-section area A of the sample. The variation of the cross-section area A during deformation must be taken into account for large strain as plastic deformation occurs at constant volume $A \cdot l$

$$A = A_0 \frac{L_0}{L_0 + \Delta L} = \frac{A_0}{1 + \varepsilon_0} \quad \dots\dots\dots(2)$$

The true normal stress where strain is uniform, is therefore given by,

$$\sigma = \frac{F}{A_0}\left(1 + \varepsilon_0\right) \quad\quad\quad\quad\quad\quad\quad (3)$$

where,

A_0 is the initial cross-sectional area and ε_0 is the engineering strain.

At room temperature, the stress-strain curve of metal is practically independent of the rate of straining attainable at ordinary testing speeds [2]. High-speed tensile tests have shown that the yield stress increases with strain rate and this effect is more pronounced at elevated temperature. The true strain rate in uni-axial is defined as,

$$\dot{\varepsilon} = \frac{V}{L} \quad\quad\quad\quad\quad\quad (4)$$

Where,

L =Current specimen height,

V =Cross head speed.

To obtain a constant strain rate during a test, it is therefore necessary to increase the platen speed proportional to the specimen height.

In earlier days, this was achieved by using a cam plastometer in which one of the compression platens is actuated by a cam of logarithmic profile. Now-a-days it is possible to achieve similar conditions using computer controlled machines.

However, if we adopt the view that the plastic response of a material can be represented in terms of a mechanical equation of state, strain-rate or strain-

acceleration sensitivity of flow stress may be determined from the tests where these quantities are allowed to vary.

As the following section shows, a displacement control test may then be interpreted in terms of strain acceleration effects.

3.2- STRAIN ACCELERTAION SENSITIVITY FROM DISPLACEMENT CONTROL TESTS.

The instantaneous strain in uni-axial test is given by,

$$d\varepsilon = \frac{dl}{l},\ \dots\dots\dots\dots\dots\dots(5)$$

Giving,

$$\varepsilon_t = \int \frac{dl}{l} = \ln(l) + c\ ,\ \dots\dots\dots\dots(6)$$

The constant c may be evaluated by imposing $\varepsilon = 0$ at $l = lo$

$$\Rightarrow 0 = \ln(lo) + c$$

Or $c = -\ln(lo)$

So, $\varepsilon_t = \ln\left(\frac{l}{lo}\right)$ $\dots\dots\dots\dots(7)$

Now, taking derivative w.r.t. time,

$$\dot{\varepsilon} = \frac{d\varepsilon_t}{dt} = \frac{d}{dt}(\ln l - \ln lo) = \frac{1}{l}\frac{dl}{dt} = \frac{V}{l}$$

$$\dot{\varepsilon} = \frac{V}{L}\ \dots\dots\dots\dots\dots(8)$$

And

$$\ddot{\varepsilon} = \frac{d\dot{\varepsilon}}{dt} = \frac{d}{dt}\left(\frac{V}{l}\right) = \frac{1}{l}\frac{dV}{dt} + V\frac{d}{dt}\left(\frac{1}{l}\right)$$

$$= 0 + V\left(\frac{-1}{l^2}\right)\frac{dl}{dt}$$

Therefore,

$$|\ddot{\varepsilon}| = \left(\frac{V}{l}\right)^2 \quad ....(9)$$

The above equation imply that a range of strain, strain rate, and strain acceleration values are achieved in a single an uni-axial test under displacement control.

The desired values can be obtained through appropriate combination of the initial length and the cross-head speed employed.

The flow-stress data obtained in this manner may then be used to obtain value of m and I (Eq.10, Chapter-1) using multiple-regression-analysis. The data beyond necking can not be used for this purpose, as the plastic deformation caused is not uniformly spread throughout the sample, but is localized.

3.3 - EXPERIMENTAL DETAILS

Experiments were conducted, on commercial purity aluminum to evaluate its strain hardening exponent and strain acceleration-sensitivity of flow stress.

Tension and compression specimen as shown in Fig 3.1 were prepared from a single piece of commercially available aluminum bar of 16-mm. dia.and 19 mm.dia.
(MTL.B)   (MTL.A)

All experiments were conducted at room temperature $(22^0 C)$ on INSTRON 1195 testing machine, interfaced with Lab View. [Data acquisition software.]

Experimental observations involved the recording of load -elongation diagram at different displacement controls (Cross-head speed) and different specimen gage lengths.

Load - elongation diagrams were plotted both on chart recorder and plotter interfaced with INSTRON 1195 machine.

Specimens have been subjected to loads both in tension and compression under displacement control in the range 0.05 to 5 mm/min. [8.33 E-4 to 0.833 mm/sec]. The gage length for tension tests were chosen from 20 to 50 mm and for compression 8 to 19 mm with aspect ratio (l / d), varying from 1 to 2.89. The details are summarized in Table 3.1.

3.3.1 RESULTS AND DISCUSSION.

Experiments have been conducted and their details are given in Table 3.1.

Fig. 3.2 shows typical load-elongation diagrams obtained in tension and compression tests. Remaining data are reported in Appendix C.

The load - elongation diagram is converted into true stress - true strain diagram to observe the strain hardening response under strain-acceleration.

To obtain true stress, true strain, and strain rate and strain acceleration from the load – elongation diagram, the approach as outlined in this chapter was followed.

A	B d (mm)	C L (mm)	D (mm/min)	m	l	F (Mpa)	G (Mpa)	Material	Ref. in Appendix C
1	4	20	0.2	0.1892	0.0031	225.2	275.0	A	a
2	5	25	1.0	0.2063	0.0024	225.2	280.2	A	b
3	10	50	1.0	0.2766	0.0054	225.6	280.2	A	c
4	4	20	0.2	0.1041	0.0156	240.2	275.0	B	d
5	5	25	1.0	0.1062	0.0145	225.1	240.1	B	e
6	6	30	0.1	0.1192	0.0148	220.7	236.6	B	f
7	8	40	0.05	0.1789	0.0166	235.9	270.0	B	g
8	7	35	5.0	0.1366	0.0175	225.5	265.0	B	h
9	9	45	2.0	0.1342	0.0131	230.7	265.1	B	i
10	10	50	0.5	0.1365	0.0167	227.3	260.0	B	j

(a) FOR TENSION TEST

A	B d (mm)	C L (mm)	D (mm/min)	m	l	F (Mpa)	G (Mpa)	Material	Ref. in Appendix C
1	12	20	0.2	0.1893	0.0094	200.5	225.1	A	k
2	12	25	0.5	0.1867	0.0099	210.5	240.3	A	l
3	17.5	35	1.0	0.1515	0.0142	210.8	262.6	A	m
4	16	40	2.0	0.1476	0.0129	215.4	262.3	A	n
5	19	55	0.2	0.1380	0.0115	200.8	218.5	A	o
6	5	8	0.2	0.1502	0.0135	201.2	236.2	A	p
7	10	10	0.2	0.1499	0.0139	210.4	255.1	A	q
8	12	12	0.5	0.1565	0.0151	200.7	260.1	A	r
9	19	19	0.5	0.2195	0.0081	199.5	207.2	A	s
10	11	15	1.0	0.1338	0.0060	250.1	280.2	B	t
11	13	15	2.0	0.1528	0.0078	240.2	266.0	B	u
12	15	22	5.0	0.1592	0.0058	245.3	273.4	B	v
13	14	20	0.5	0.1822	0.0036	235.1	280.0	B	w
14	5	8	0.2	0.1753	0.0033	250.0	272.5	B	x
15	9	10	0.1	0.2104	0.0079	240.3	281.2	B	y
16	7	10	0.05	0.2114	0.0007	231.0	285.1	B	z

(b) FOR COMPRESSION TEST

Note: A: SNo.   F: Yield stress
         B: Diameter   G: Ultimate tensile strength
         C: Gage length   m: Strain-hardening exponent
         D: Cross-head speed l: Strain-acceleration sensitivity of flow stress

Table 3.1   **Experimental Details and Results**

Fig.3.3-3.6 shows typical diagrams of,

1. Engineering stress - Engineering strain (Fig 3.3)

2. True stress - True strain (Fig.3.4)

3. True stress - true plastic strain (Fig.3.5)

4. Variation of flow stress with strain acceleration (Fig.3.6)

The true stress - true strain curve is similar in nature, to one given in Figure 1.1

True plastic strain has continuously increased with true stress.

Typical relationship between true stress, true strain and strain acceleration

is illustrated in Fig.3.7.

Best values of parameters m and I (Eq.10, Chapter 1) were determined for

each test using the procedure outlined in Appendix A. The values are typically, m

= 0.15 to 0.21 and I = 0.005 to 0.015 and the constitutive law is,

$$\sigma = 43.32\varepsilon^{0.18}\dot{\varepsilon}^{0.01},$$

The strain-hardening exponent is in good agreement with the literature

value (Table 1.1, Chapter 1)

3.4 REFERENCES :

1. Poirier J.N., "Creep of Crystals.", Cambridge Univ. Press.,1985.

2. Chakraborty J. "Theory of Plasticity." McGraw-Hill International.,1987.
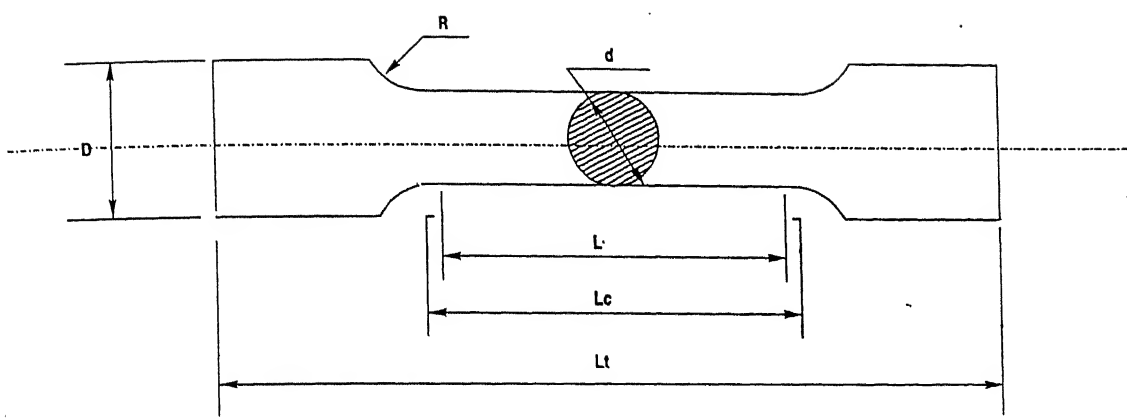
GAUGE LENGTH	DIAMETER	DIAMETER	MINIMUM PARALLEL	TOTAL LENGTH Lt	RADIUS
L	d	D	LENGTH Lp		R

SPECIMEN FOR TENSION TEST
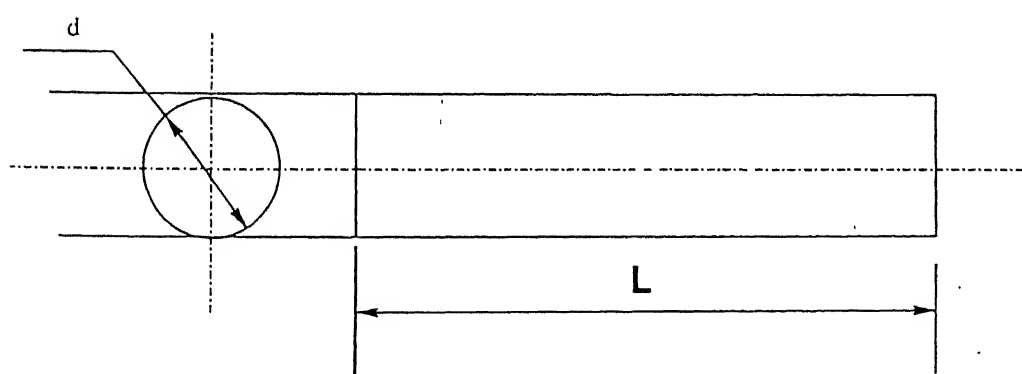
SPECIMEN FOR COMPRESSION TEST

Figure 3.1   Schematic diagrams showing tension and Compression specimen.
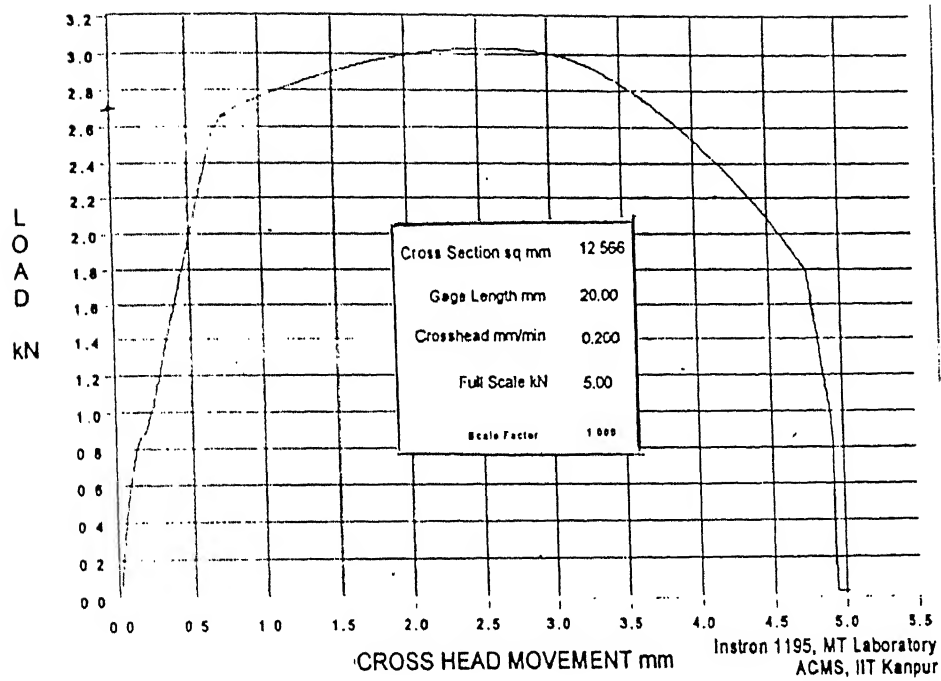
(a)
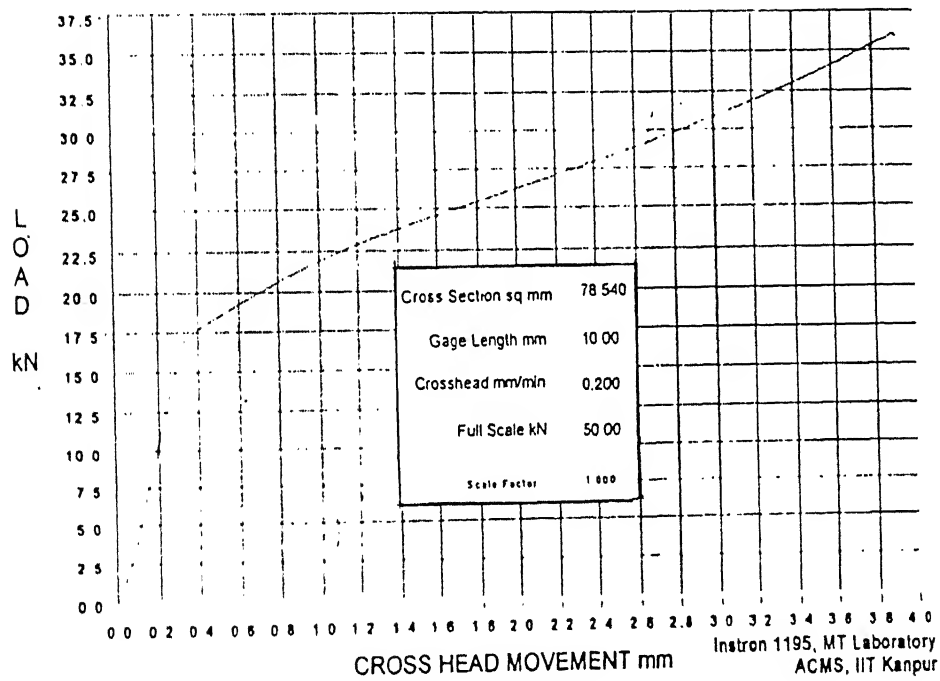
(b)

Figure 3.2   Typical load-elongation diagrams obtained in (a) tension
and (b) compression of aluminium specimen
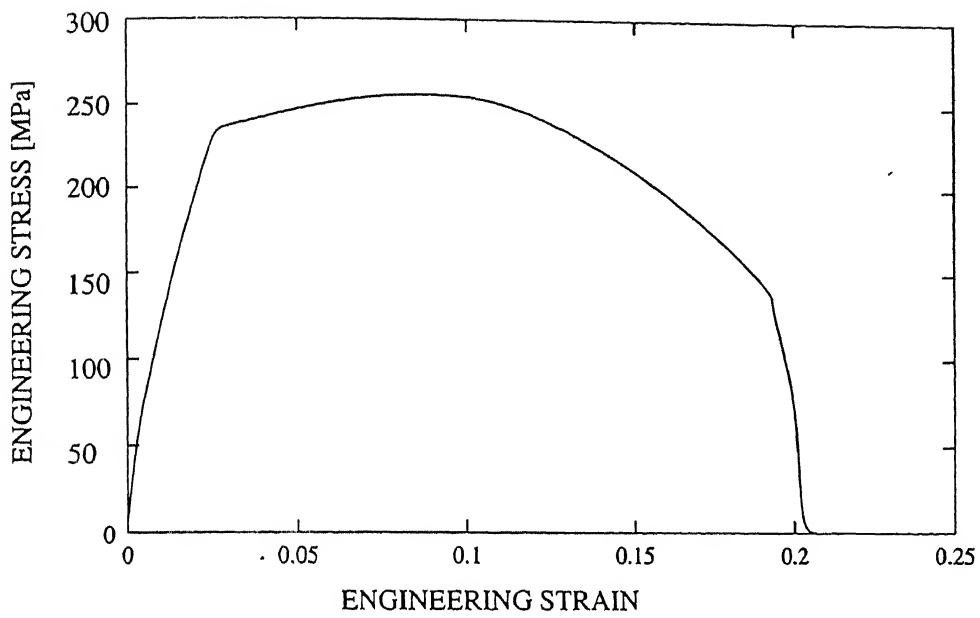
Figure 3.3   Engineering stress/strain curve based on figure 3.2(a).
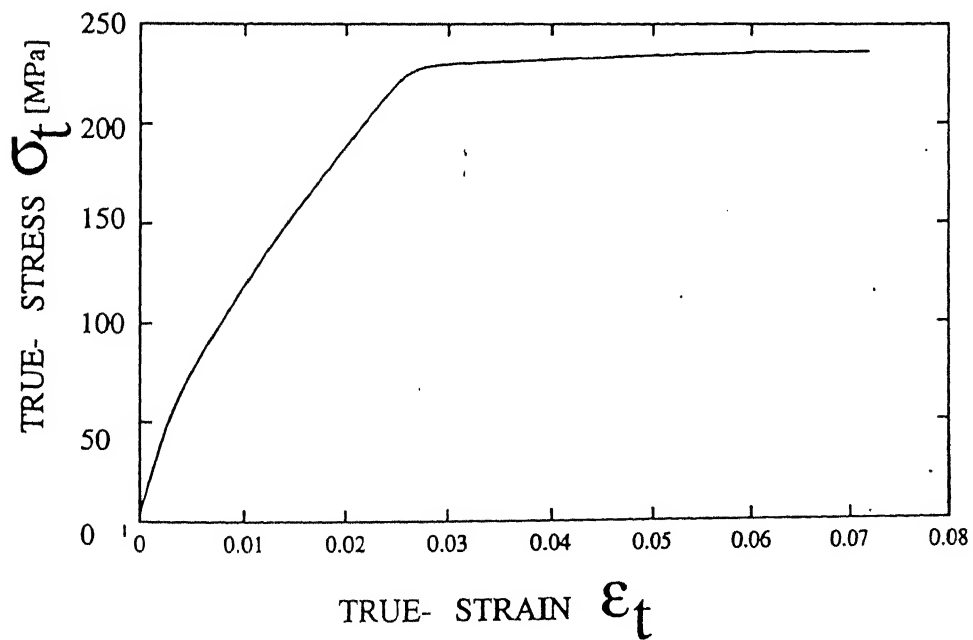
Figure 3.4   True stress/strain curve based on figure 3.3.
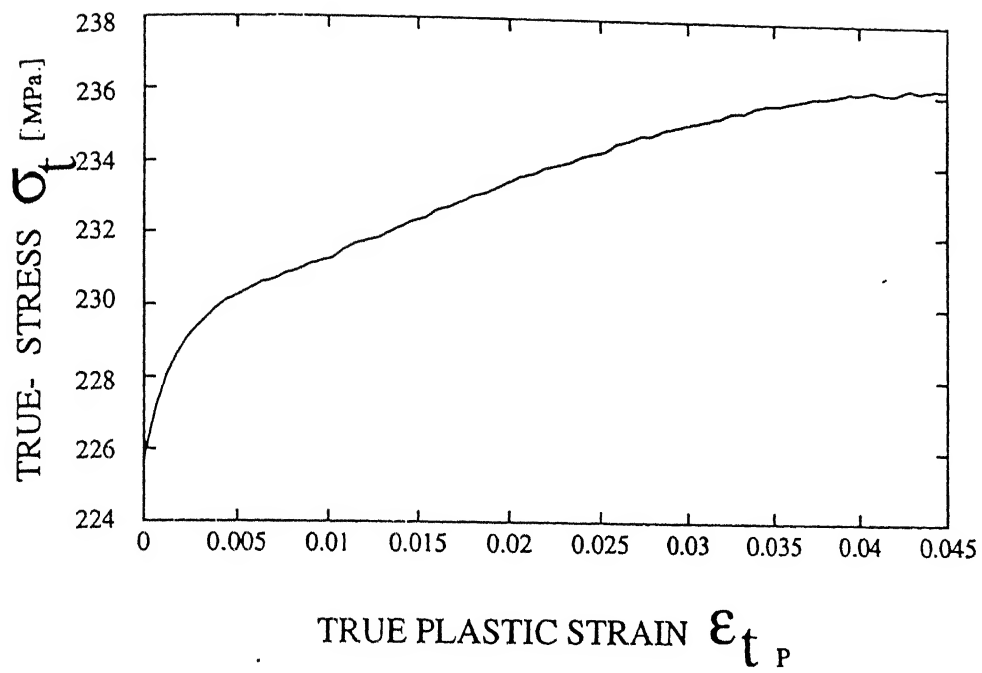
Figure 3.5   True stress/plastic-strain curve based on figure 3.4.
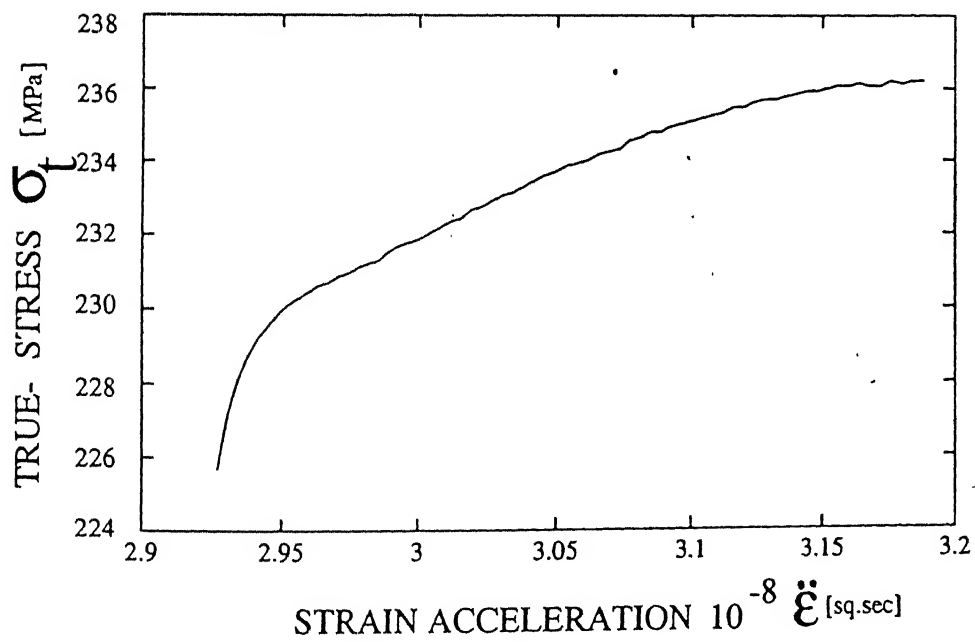
Figure 3.6   Variation of flow stress with strain-acceleration based on figure 3.5.
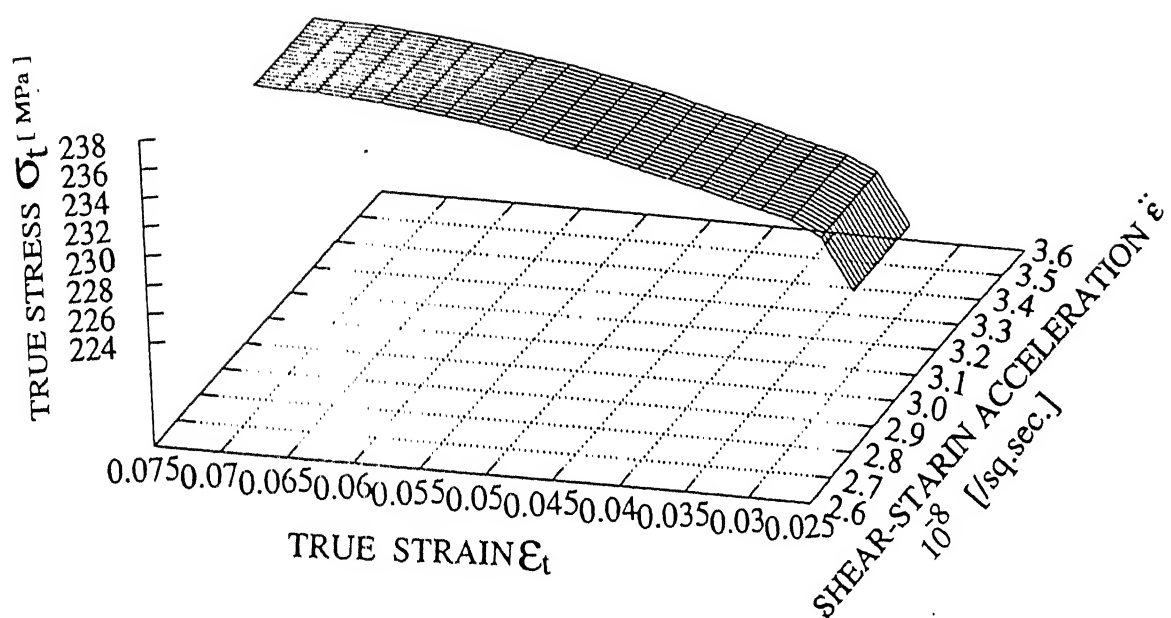
Figure 3.7   Variation of flow stress with strain and strain acceleration.

CHAPTER 4

CONCLUSIONS AND FUTURE WORK.

4.1 CONCLUSIONS.

This work has dealt with the effect of strain acceleration on plastic deformation behavior of aluminium. As described in the preceeding chapters the phenomenon was studied using both uni-axial specimen and the more complex situation of metal cutting. The effec of strain and strain-acceleration on the flow stress of aluminium was then quantified in terms of an empirical power-law expression proposed in this work. Table 4.1 lists the form of the equations and the values of the strain hardening exponents and strain acceleration sensitivities.

We can draw the following conclusions, based on this work:

(a) We propose the following equations:

$$\sigma = 35.49\,\varepsilon^{0.23}\,\ddot{\varepsilon}^{0.017} \qquad \textit{for machining}$$
$$\sigma = 44\varepsilon^{0.18}\,\ddot{\varepsilon}^{0.017} \qquad \textit{for uni - axial loading}$$

for strain and strain acceleration dependence of flow stress in aluminium.

(b) The strain hardening exponents obtained through uni-axial tests and machining tests are in good agreement with values available in the literature.

(c) Even though the range of strain and strain-acceleration values for uni-axial test and machining test differ by an order of magnitude, the parameters m and I have similar values for the two tests. This suggests that the constitutive equation proposed may be applicable more generally.

Table 4.1 COMPARISON TABLE

	Machining Tests.	Uni-axial Tension.	Uni-axial Compression.	Literature Values.
Constitutive equation.	$\sigma_s = k\gamma^m \dot{\gamma}^l$ (proposed)	$\sigma = k\varepsilon^m \dot{\varepsilon}^l$ (proposed)	$\sigma = k\varepsilon^m \dot{\varepsilon}^l$ (proposed)	$\sigma = k\varepsilon^m$
Range of $\dot{\varepsilon}$ values used.	2.17-8.07 [/sec]	0.019-0.262 [/sec]	0.019-0.262 [/sec]	-
Range of $\ddot{\varepsilon}$ values used.	0.0024-0.2082 [/sq.sec]	1.1E-7 –9.8E-8 [/sq.sec]	1.06E-7-9.8E-8 [/sq.sec]	-
k	35.49	44.00	44.00	44.00
m	0.230	o.189	0.182	0.211
l	0.017	0.017	0.015	-

4.2 SCOPE FOR FUTURE WORK.

1. The phenomenon may be studied using computer-controlled machines, which may enable constant strain-acceleration during a uni-axial test.

2. Results of high strain hardening materials, viz. copper, steels and others should be compared with low hardening materials, viz. molybdenum and titanium in concern with the strain acceleration sensitivity so as test the validity of the proposed power law over a range of materials with different plastic behavior.

3. More experiments can be conducted on other ferrous and non-ferrous materials to analyze the effect of strain acceleration on flow stress.

4. The physical basis of strain-acceleration sensitivity of flow stress needs to be studied in terms of the associated deformation mechanisms.

APPENDIX : A

$$\boxed{\text{START}}$$

INPUT
INITIAL AREA (Ao) , ORIGINAL GAGE LENGTH (Lo), CROSS-HEAD SPEED (v),
ELONGATION STEP (E), LOAD (P), k AT ρ=1
FROM INSTRON 1195, MACHINE DATA FILE.

DO i=1 TO n

IS i>n ──YES──→ (B)

NO

STUCTURE   VALUE(n)

VALUE.ELONGATION=n E

VALUE.LENGTH_ACTUAL=Lo-n.E

$$\text{VALUE.AREA\_ACTUAL} = \frac{Ao.Lo}{\text{VALUE.LENGTH\_ACTUAL}}$$

$$\text{VALUE.TRUE\_STRESS} = \frac{LOAD}{\text{VALUE.AREA\_ACTUAL}}$$

$$\text{VALUE.STRAIN\_RATE} = \frac{\text{CROSS HEAD VELOCITY}}{\text{VALUE.STRAIN\_RATE}}$$

VALUE.STRAIN_ACCELERATION= (VALUE.STRAIN_RATE)**2

i=i+1

(A)

$$q = k \, \varepsilon_1^m \, \ddot{\varepsilon}_1^l$$

q = TRUE STRESS

ε_1 = TRUE STRAIN

$\ddot{\varepsilon}_1$ = STRAIN ACCELERAION.

m= STRAIN HARDENING COEFFICIENT.

(B)

SELECT STRESS AT NECKING
AND YIELD POINT (AT 0.2 % OF MAXIMUM STRESS FOR ALUMINIUM)
FORM STRUCTURE------- VALUE.TRUE   _STRESS(n)

j=No.Of DATA BETWEEN YIELD POINT AND NECKING.
REASSIGN THE VALUES FROM YIELD POINT TO NECKING POINT.
TO TRUE_STRESS, TRUE_STRAIN AND STRAIN_ACCELERATION.

DO i=1 TO J
TRUE_PLASTIC_STRESS=TRUE_STRESS(J)-STRAIN_YIELD

(A)

EQUATION $q = k \, \varepsilon_1^m \, \ddot{\varepsilon}_1^l$

$LOG \, q = LOG \, k + m \, LOG \, \ddot{\varepsilon}_1 + l \, LOG \, \ddot{\varepsilon}_1$

APPLY LEAST SQUATE METHOD

$\Sigma \, LOG \, \frac{q}{k} \, LOG \varepsilon_1 = m \, \Sigma \, LOG \varepsilon_1 . LOG \, \varepsilon_1 + l \, \Sigma \, (LOG \, \ddot{\varepsilon}_1).(LOG \, \ddot{\varepsilon}_1)$

$\Sigma \, LOG \, \frac{q}{k} \, LOG \ddot{\varepsilon}_1 = m \, \Sigma \, LOG \, \varepsilon_1 . LOG \, \ddot{\varepsilon}_1 + l \, \Sigma \, (LOG \, \ddot{\varepsilon}_1).(LOG \, \ddot{\varepsilon}_1$

APPLY METHOD OF GAUSS ELIMINATION

GET VALUES m, l

$$\boxed{\text{STOP}}$$

APPENDIX B

A

Records of forces from the experiments.

Diameter 16 mm., without coolant

FOR (a) CUTTING FORCE

FOR (b) FEED FORCE

1 div = 0.05 mV.

7 divs = .35 mV.
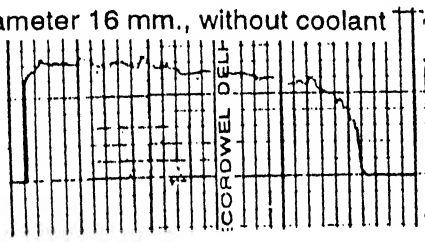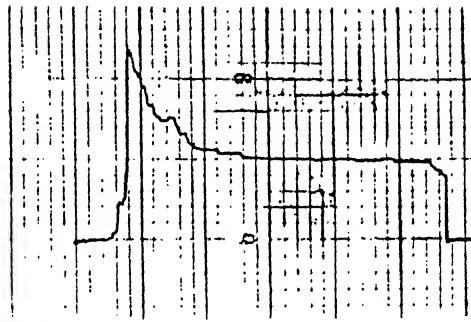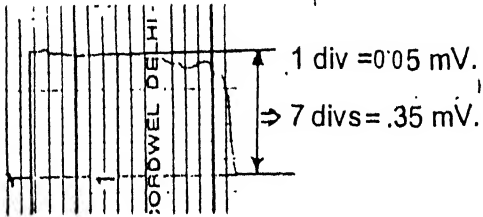
EXPERIMENTAL DETAILS

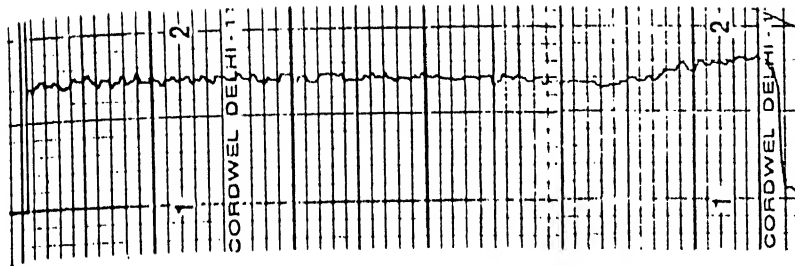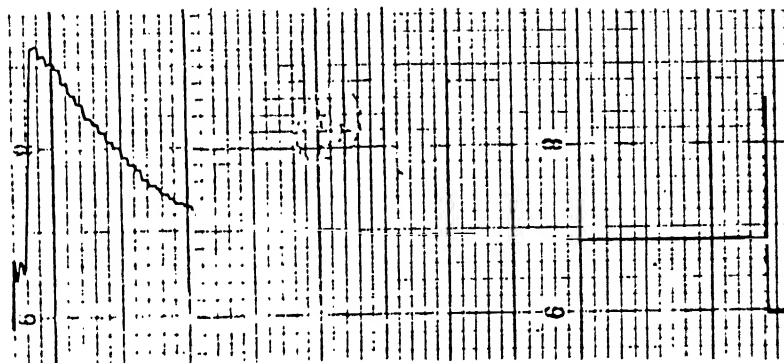| SR. NO	'f' FEED [mm/rev]	'N' SPINDLE SPEED [rpm]
1	0.042	80.
2	0.042	250
3	0.083	80.
4	0.083	250
5	0.066	40.
6	0.066	320
7	0.100	200
8	0.066	200
9	0.066	200
10	0.066	200
11	0.066	200
12	0.066	200
13	0.066	200.

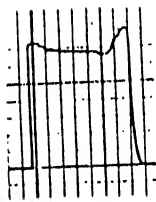NOTE: ALL THE RECORD ARE AT 5 milli-volt FULL-SCALE.,

6

6

7

7

8

8

9

9

10

10
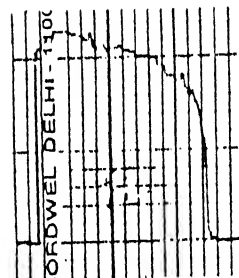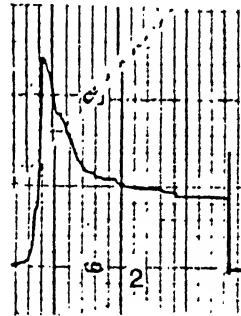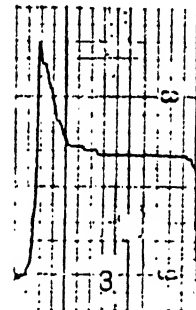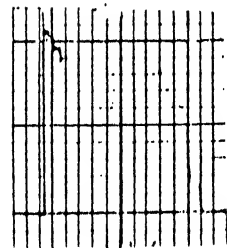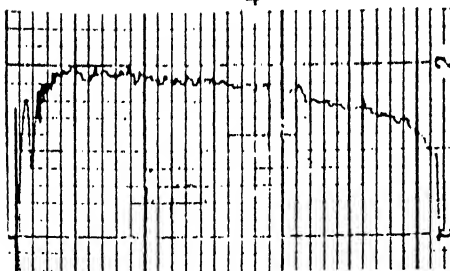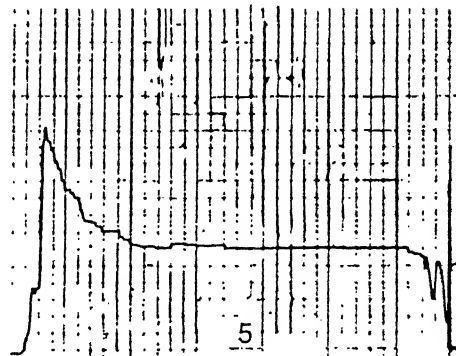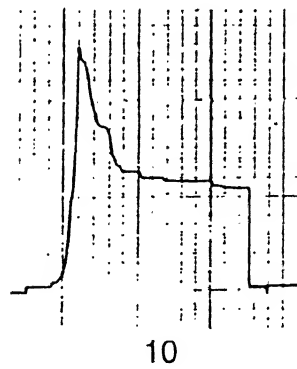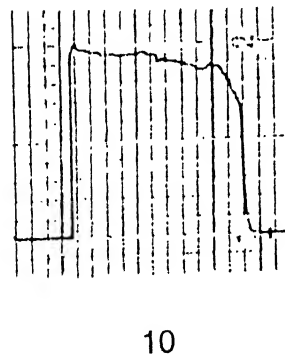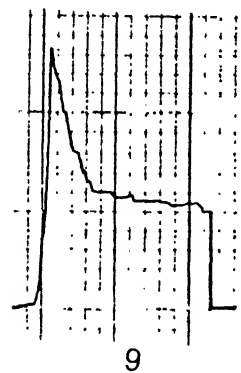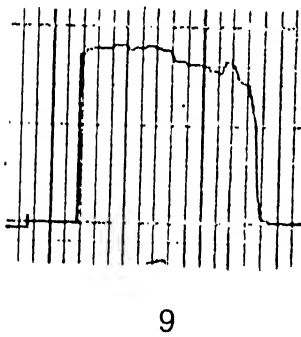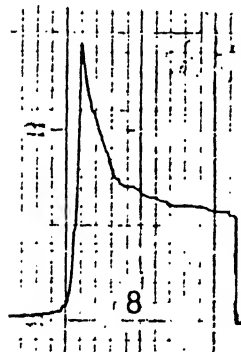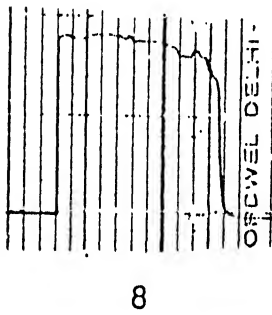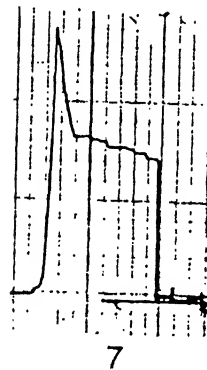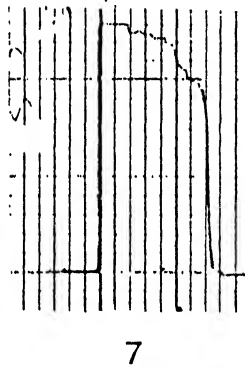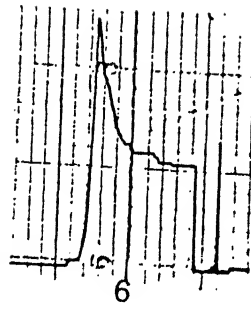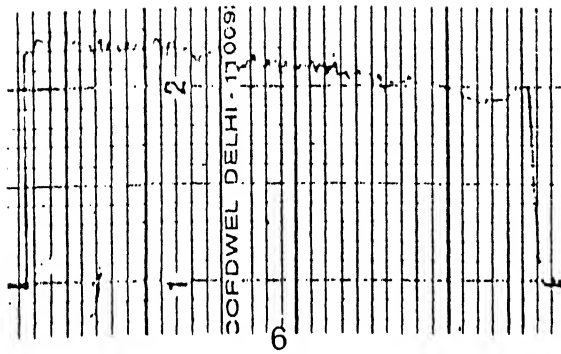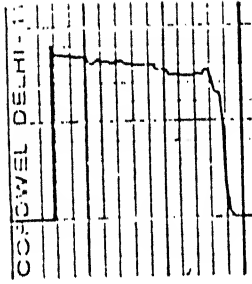
11
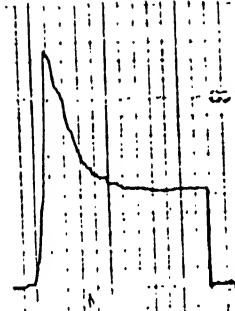
11
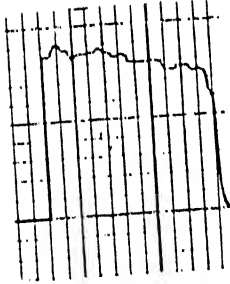
12
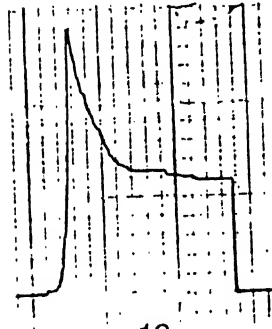
12

13
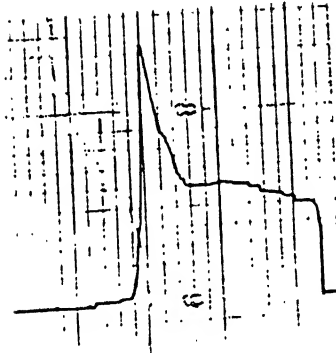
13·

Records of forces from the experiments.

B. Diameter 16 mm., with coolant
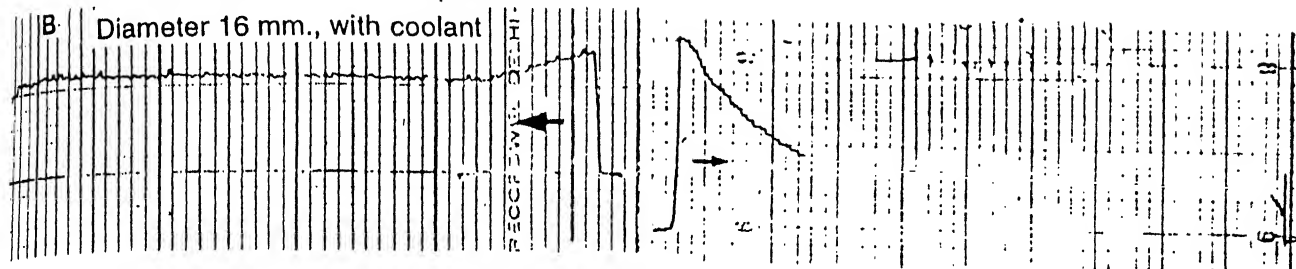
(a)

(b)

FOR (a)
CUTTING FORCE
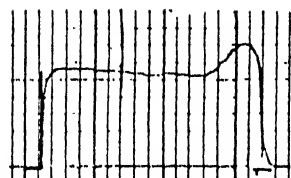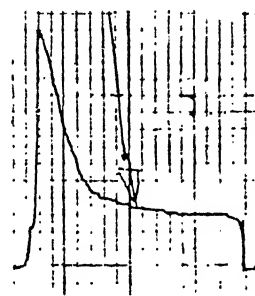
FOR (b)
FEED FORCE
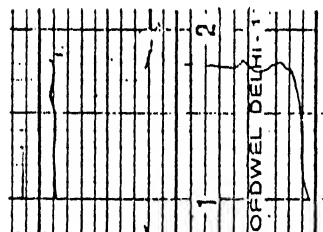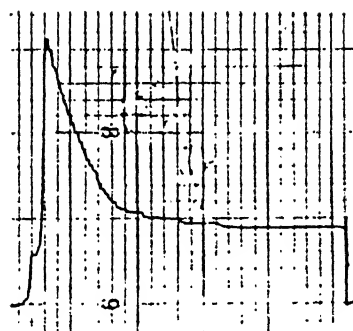
EXPERIMENTAL DETAILS

SR. NO	FEED 'f' [mm/rev.]	SPIN SPED 'N' [rpm]
1	0.042	80
2	0.042	250
3	0.083	80
4	0.083	250
5	0.066	40
6	0.066	320
7	0.100	200
8	0.066	200

NOTE: ALL THE RECORD ARE AT 5 milli-volt FULL-SCALE.

CORDWEL DELHI · 1

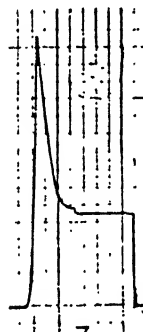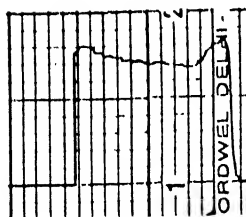CORDWEL DELHI

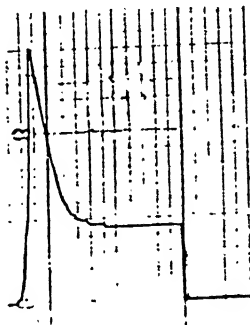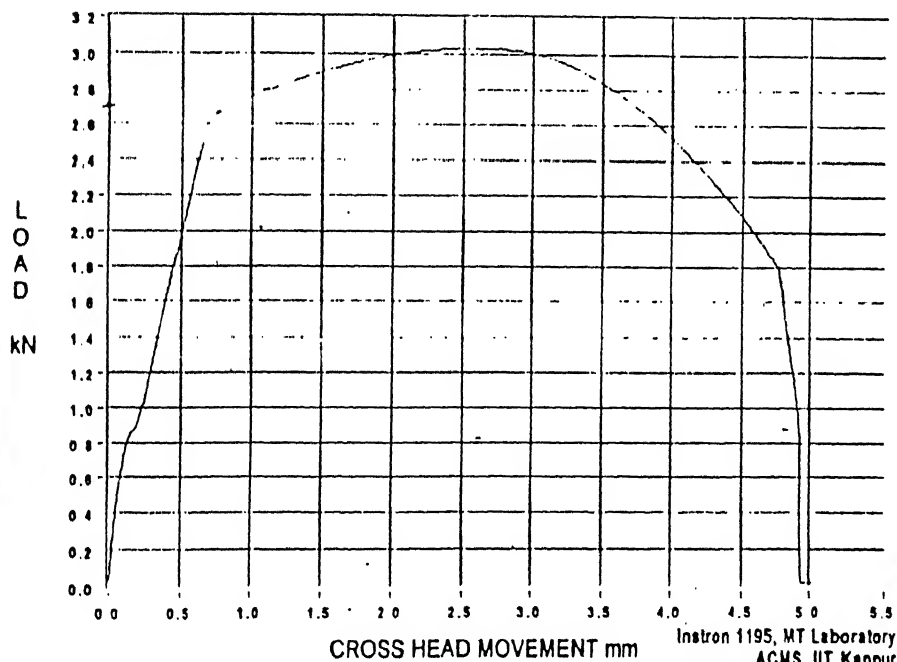5

5

6

6

7

7

CORDWEL DELHI
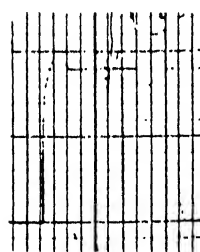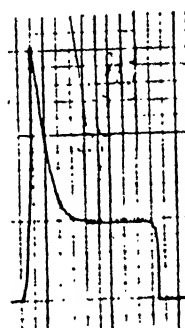
8

8

APPENDIX C

Load-elongation diagrams obtained in tension and compression of aluminum specimen.

TENSION TEST ON ALUMINIUM 1   17/08/98   16:16   a
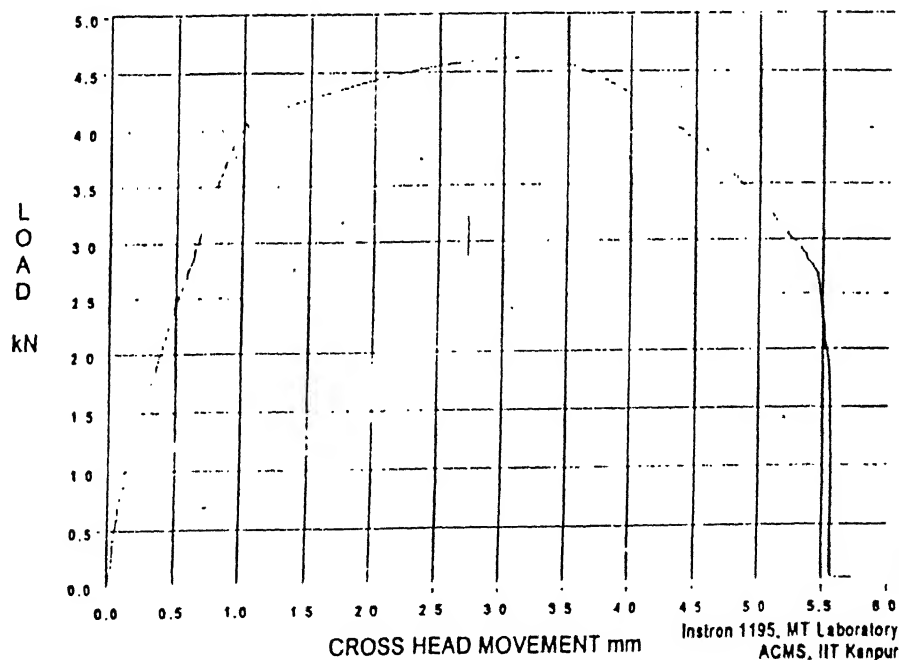
FILE \ C:\DATA\INSTRON\N081700.TXT

Cross Section sq.mm	12.566
Gage Length mm	20.00
Crosshead mm/min	0.200
Full Scale kN	5.00
Scale Factor	1.000

LOAD kN vs CROSS HEAD MOVEMENT mm

Instron 1195, MT Laboratory
ACMS, IIT Kanpur

TENSION TEST ON ALUMINIUM 2   17/08/98   16:45   b

FILE \ C:\DATA\INSTRON\N081701.TXT

Cross Section sq.mm	19.635
Gage Length mm	25.00
Crosshead mm/min	1.000
Full Scale kN	5.00
Scale Factor	1.000

LOAD kN vs CROSS HEAD MOVEMENT mm

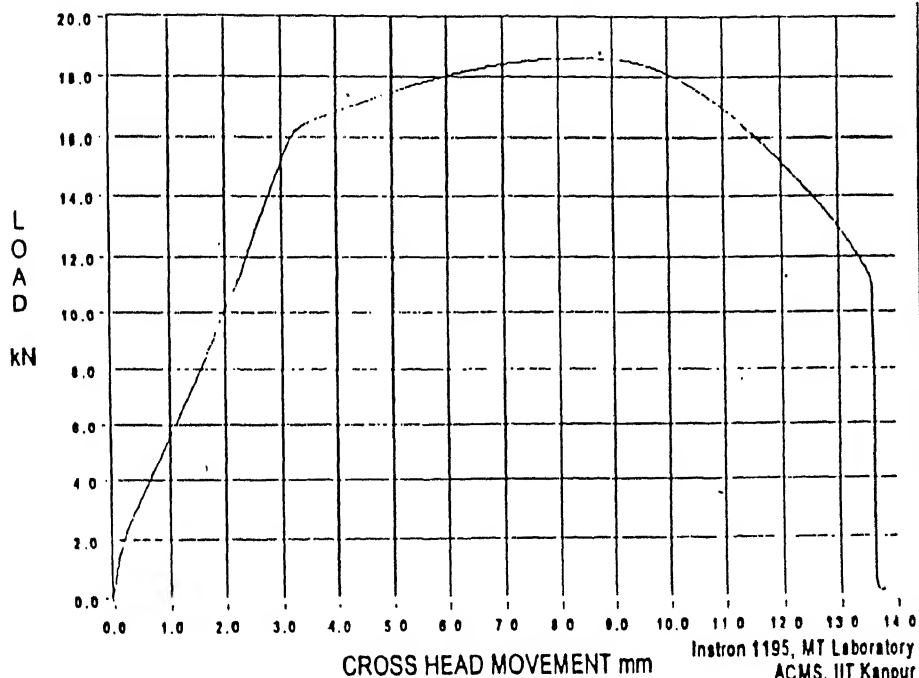Instron 1195, MT Laboratory
ACMS, IIT Kanpur

TENSION TEST ON ALUMINIUM 3   17/08/98   16:56   C

FILE C:\DATA\INSTRON\N081702.TXT

Cross Section sq.mm	78.540
Gage Length mm	50.00
Crosshead mm/min	1.000
Full Scale kN	50.00
Scale Factor	1.000

LOAD kN

CROSS HEAD MOVEMENT mm

Instron 1195, MT Laboratory
ACMS, IIT Kanpur

TENSION TEST ON ALUMINUM 1   07/10/98   10:35   d

FILE C:\DATA\INSTRON\N100702.TXT

Cross Section sq.mm	12.566
Gage Length mm	20.00
Crosshead mm/min	0.200
Full Scale kN	10.00
Scale Factor	1.000

LOAD kN

CROSS HEAD MOVEMENT mm

Instron 1195, MT Laboratory
ACMS, IIT Kanpur

TENSION TEST ON ALLUMINUM 2   07/10/98   11:01   ℰ

Cross Section sq.mm	19.635
Gage Length mm	25 .00
Crosshead mm/min	1.000
Full Scale kN	10.00
Scale Factor	1.000

LOAD kN vs CROSS HEAD MOVEMENT mm

Instron 1195, MT Laboratory
ACMS, IIT Kanpur
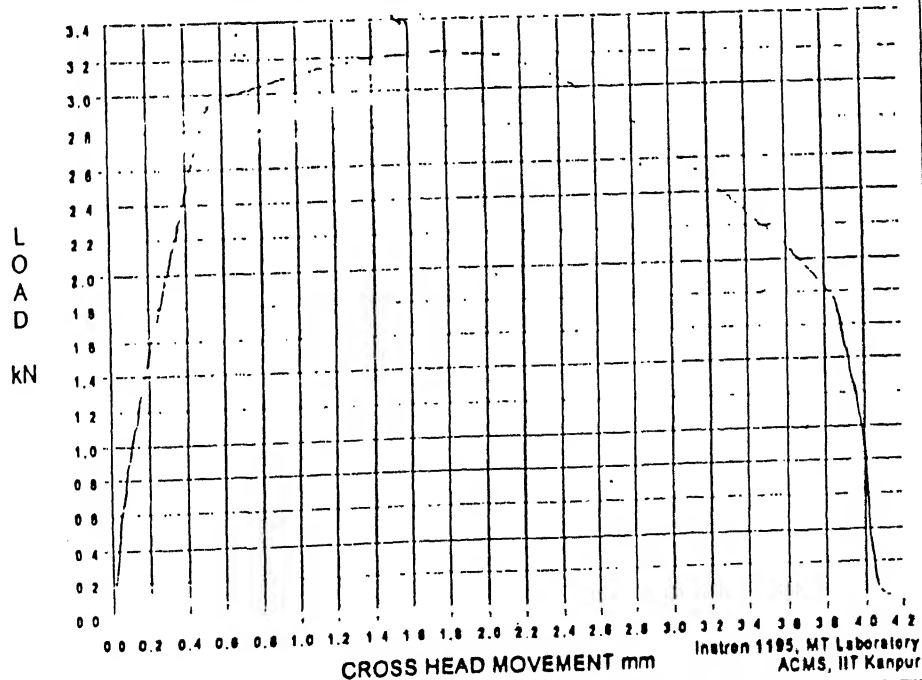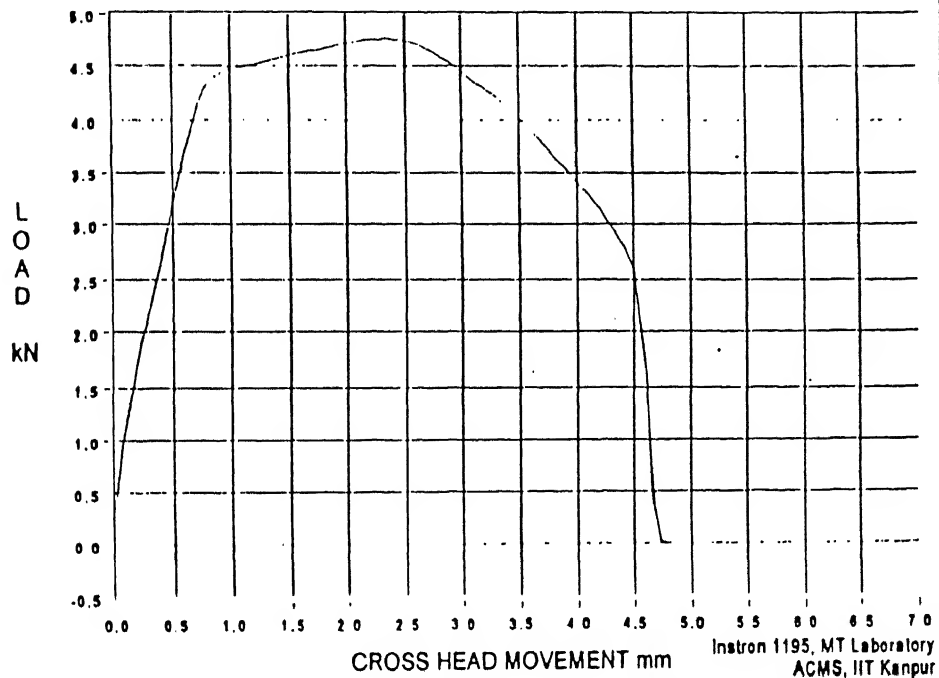
TENSION TEST ON ALLUMINUM 3   07/10/98   11:26   ƒ

Cross Section sq.mm	28.274
Gage Length mm	30.00
Crosshead mm/min	0.100
Full Scale kN	20.00
Scale Factor	1.000

LOAD kN vs CROSS HEAD MOVEMENT mm

Instron 1195, MT Laboratory
ACMS, IIT Kanpur
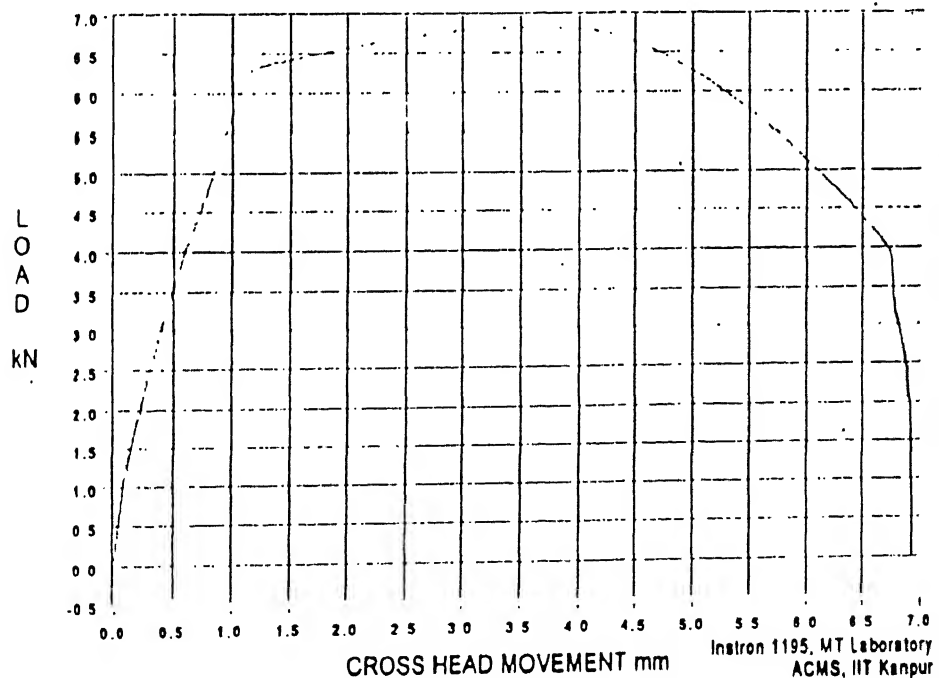
TENSION TEST ON ALLUMINUM 5   07/10/98   12:41   g

FILE : C:\DATA\INSTRON\N100705.TXT

Cross Section sq.mm	50.265
Gage Length mm	40.00
Crosshead mm/min	0.050
Full Scale kN	20.00
Scale Factor	1.000

LOAD kN vs CROSS HEAD MOVEMENT mm

Instron 1195, MT Laboratory
ACMS, IIT Kanpur
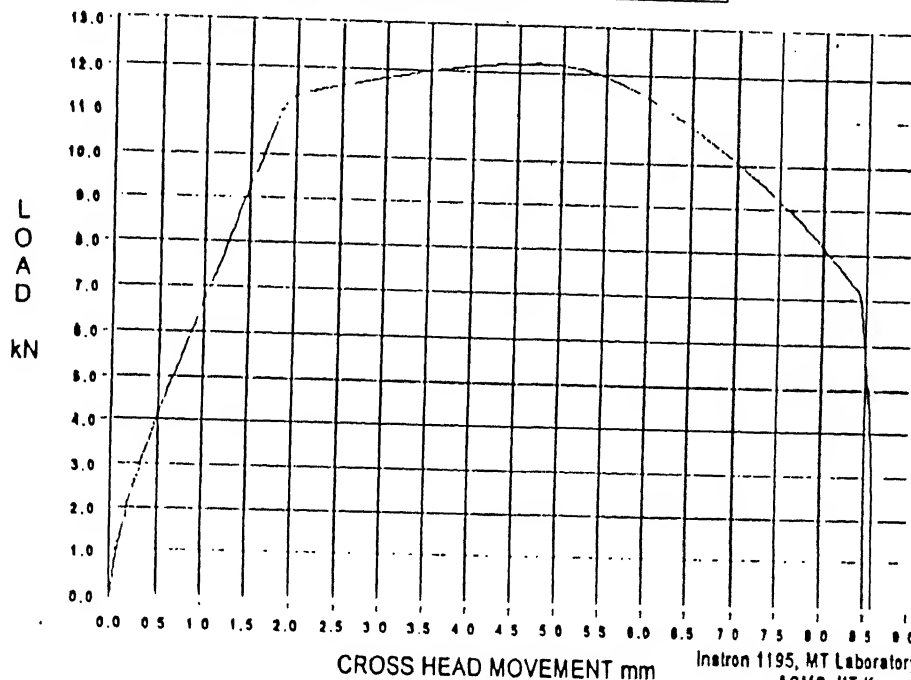
TENSION TEST ON ALLUMINUM 4   07/10/98   15:39   h

FILE : C:\DATA\INSTRON\N100706.TXT

Cross Section sq.mm	38.485
Gage Length mm	35.00
Crosshead mm/min	5.000
Full Scale kN	20.00
Scale Factor	1.000

LOAD kN vs CROSS HEAD MOVEMENT mm

Instron 1195, MT Laboratory
ACMS, IIT Kanpur
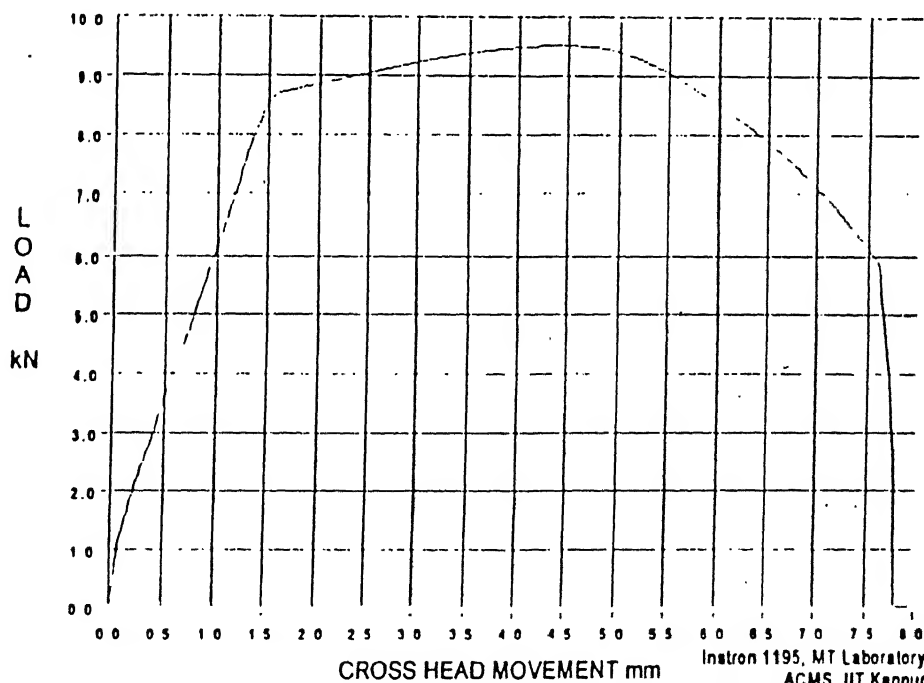
TENSION TEST ON ALLUMINUM 6   07/10/98   15:46   L

FILE \ C:\DATA\INSTRON\N100707.TXT

Cross Section sq.mm	63.617
Gage Length mm	45.00
CrossHead mm/min	2.000
Full Scale kN	50.00
Scale Factor	1.000

LOAD kN vs CROSS HEAD MOVEMENT mm

Instron 1195, MT Laboratory
ACMS, IIT Kanpur
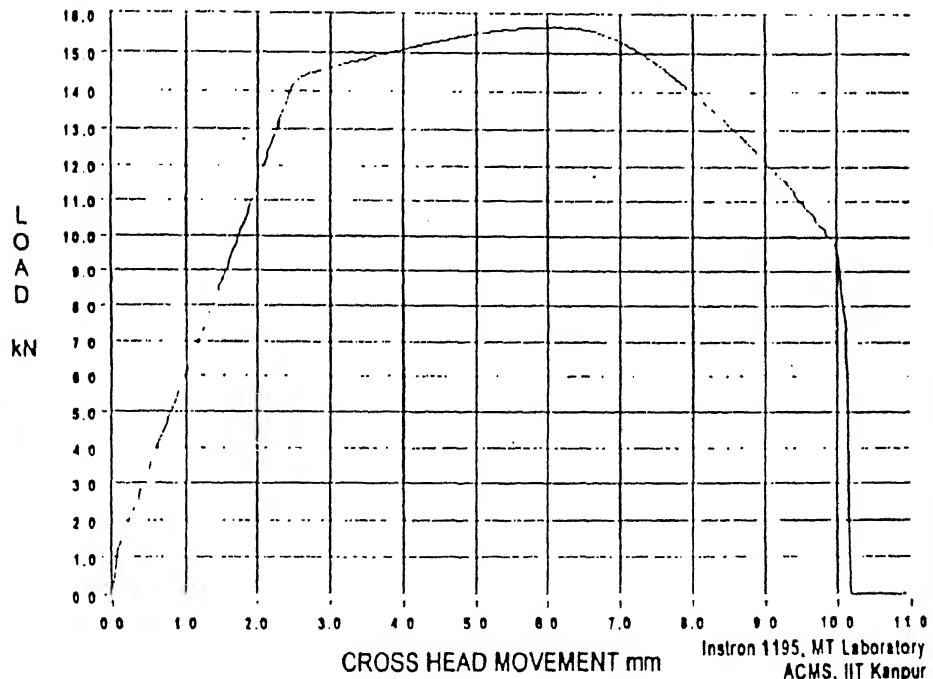
TENSION TEST ON ALLUMINUM 7   07/10/98   15:56   J

FILE \ C:\DATA\INSTRON\N100708.TXT

Cross Section sq.mm	78.540
Gage Length mm	50.00
Crosshead mm/min	0.500
Full Scale kN	50.00
Scale Factor	1.000

LOAD kN vs CROSS HEAD MOVEMENT mm

Instron 1195, MT Laboratory
ACMS, IIT Kanpur
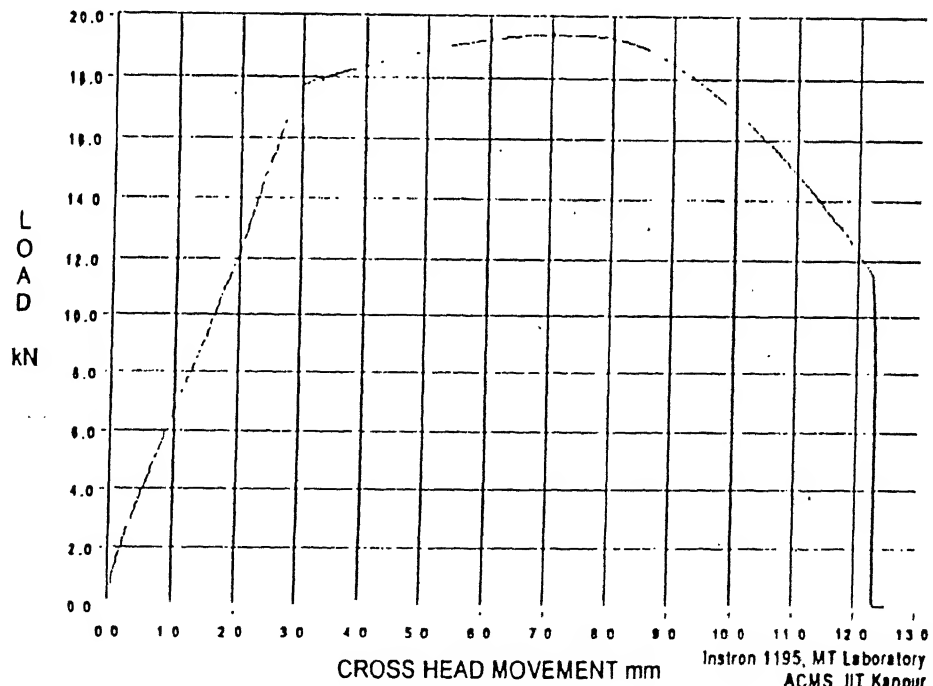
Compression Test of Aluminium 02/09/98 10:30 k

Cross Section sq.mm	113.097
Gage Length mm	20.00
Crosshead mm/min	0.200
Full Scale kN	50.00
Scale Factor	1.000

LOAD kN

CROSS HEAD MOVEMENT mm
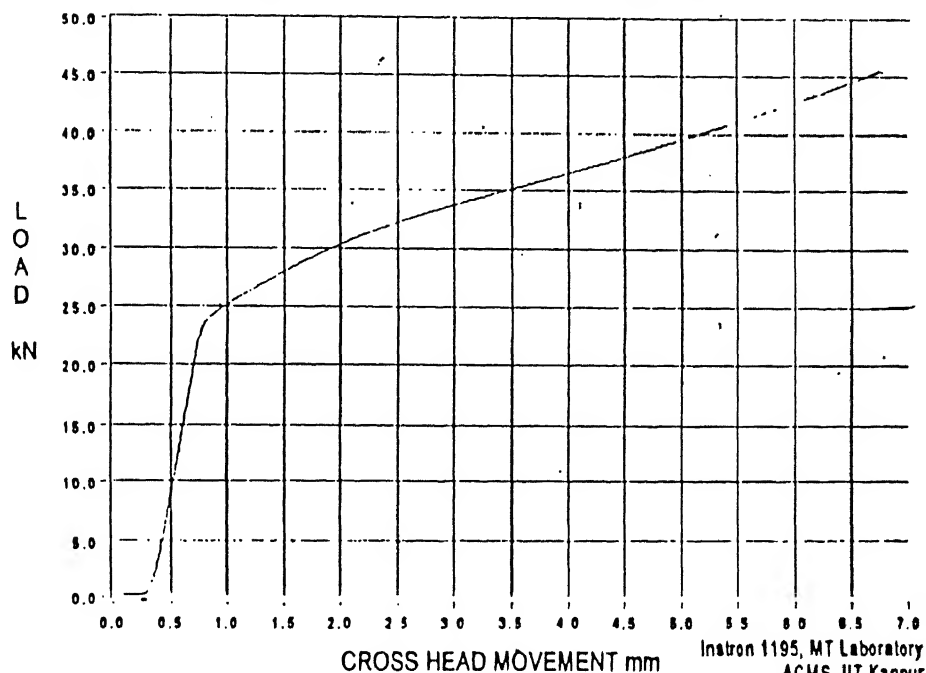
Instron 1195, MT Laboratory
ACMS, IIT Kanpur

Compression Test of Aluminium 02/09/98 11:09 ℓ

FILE \ C:\DATA\INSTRON\N090201.TXT

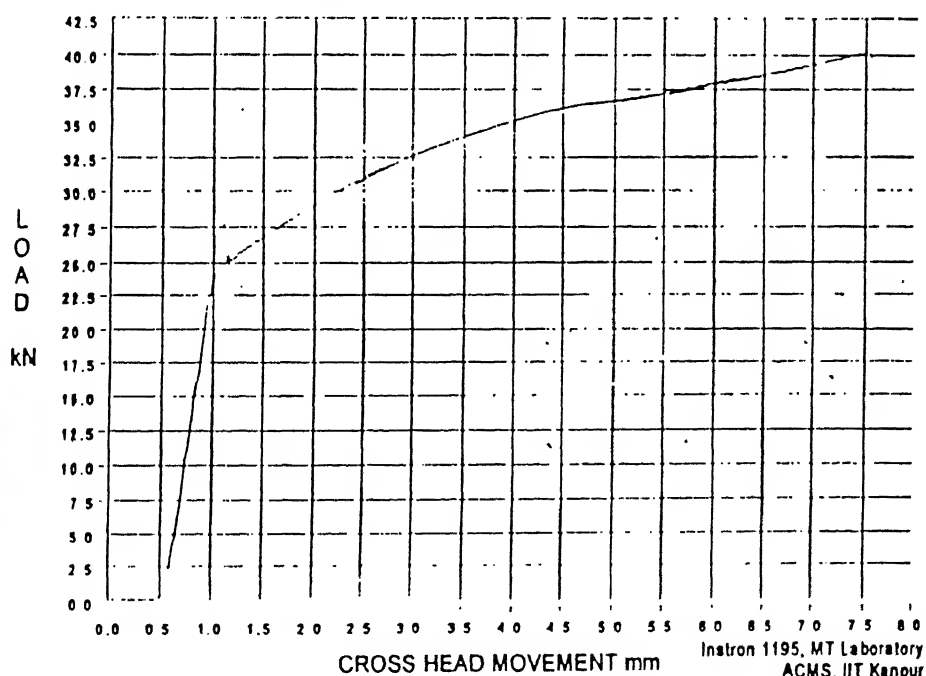|	
Cross Section sq.mm	113.097
Gage Length mm	25.00
Crosshead mm/min	0.500
Full Scale kN	50.00
Scale Factor	1.000

LOAD kN

CROSS HEAD MOVEMENT mm

Instron 1195, MT Laboratory
ACMS, IIT Kanpur

Compression Test of Aluminium   02/09/98   11:29   m

FILE : C:\DATA\INSTRON\N090202.TXT

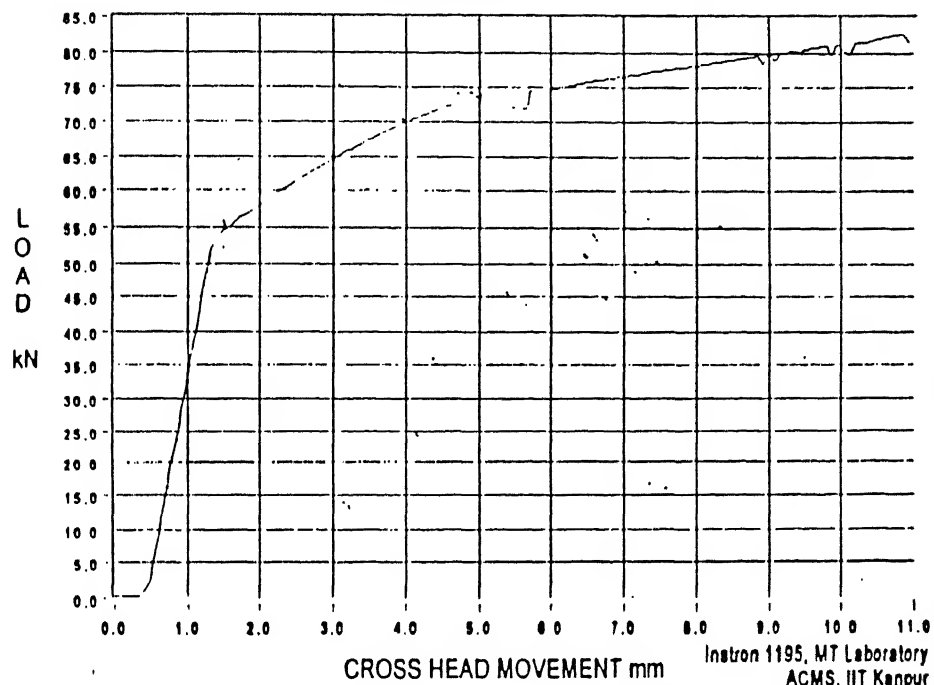| Cross Section sq.mm | 240.528 |
Gage Length mm	35.00
Crosshead mm/min	1.000
Full Scale kN	100.00
Scale Factor	1.000

LOAD kN

CROSS HEAD MOVEMENT mm

Instron 1195, MT Laboratory
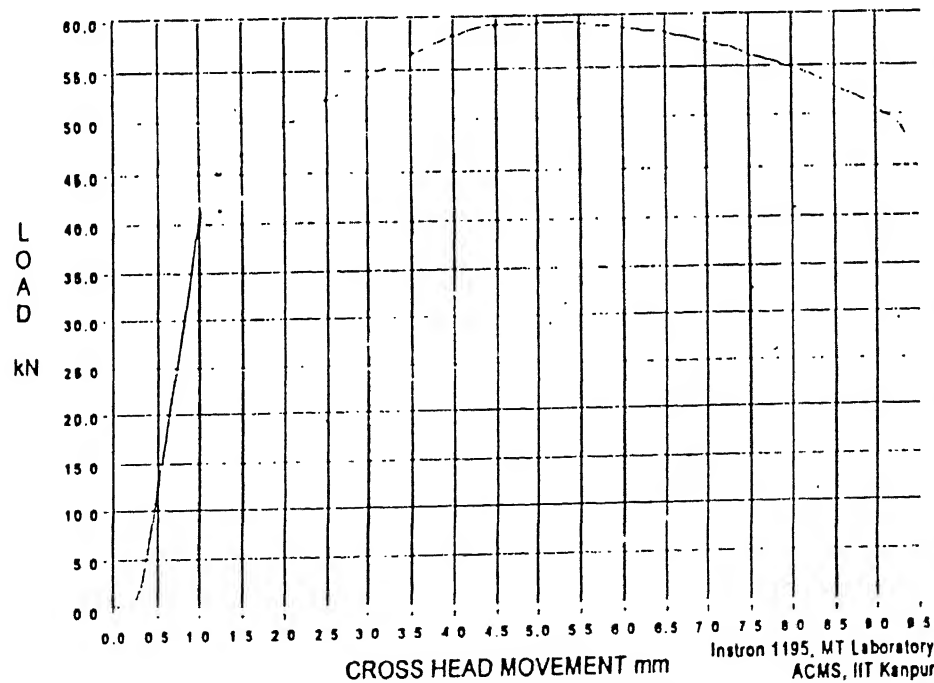ACMS, IIT Kanpur

Compression Test of Aluminium   02/09/98   11:49   n

FILE : C:\DATA\INSTRON\N090203.TXT

Cross Section sq.mm	201.062
Gage Length mm	40.00
Crosshead mm/min	2.000
Full Scale kN	100.00
Scale Factor	1.000

LOAD kN

CROSS HEAD MOVEMENT mm

Instron 1195, MT Laboratory
ACMS, IIT Kanpur

Compression Test of Aluminium   02/09/98   11:59   O

FILE ⁰⁄₀ C:\DATA\INSTRON\N090204.TXT

Cross Section sq.mm	283.529
Gage Length mm	55.00
Crosshead mm/min	0.200
Full Scale kN	100.00
Scale Factor	1.000

LOAD kN

CROSS HEAD MOVEMENT mm

Instron 1195, MT Laboratory
ACMS, IIT Kanpur

---
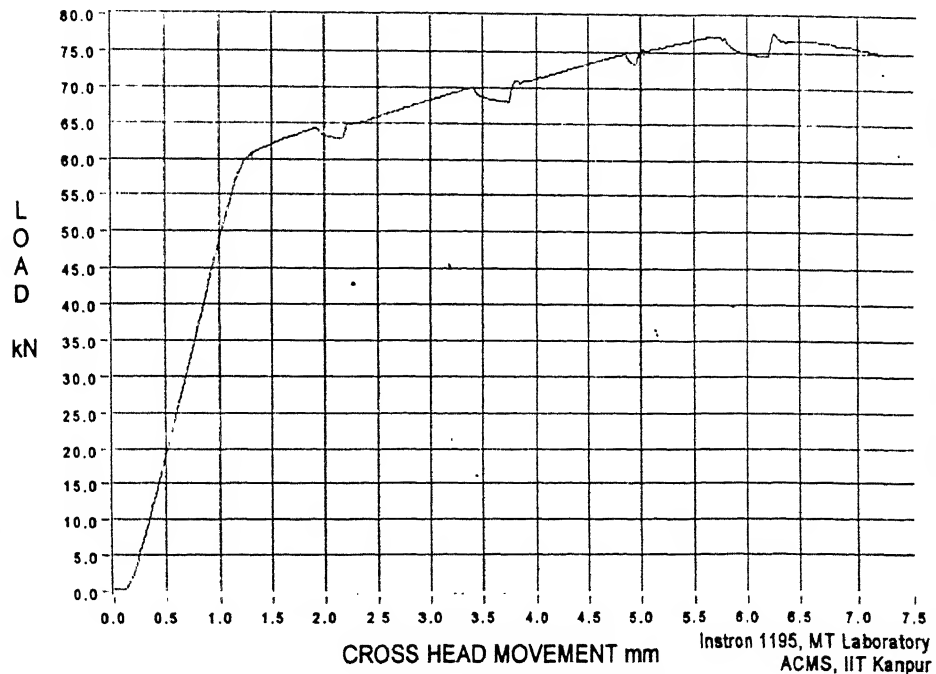
compression of aluminium sample   03/09/98   14:30   P

FILE ⁰⁄₀ C:\DATA\INSTRON\N090300.TXT

Cross Section sq.mm	19.635
Gage Length mm	8.00
Crosshead mm/min	0.200
Full Scale kN	5.00
Scale Factor	1.000
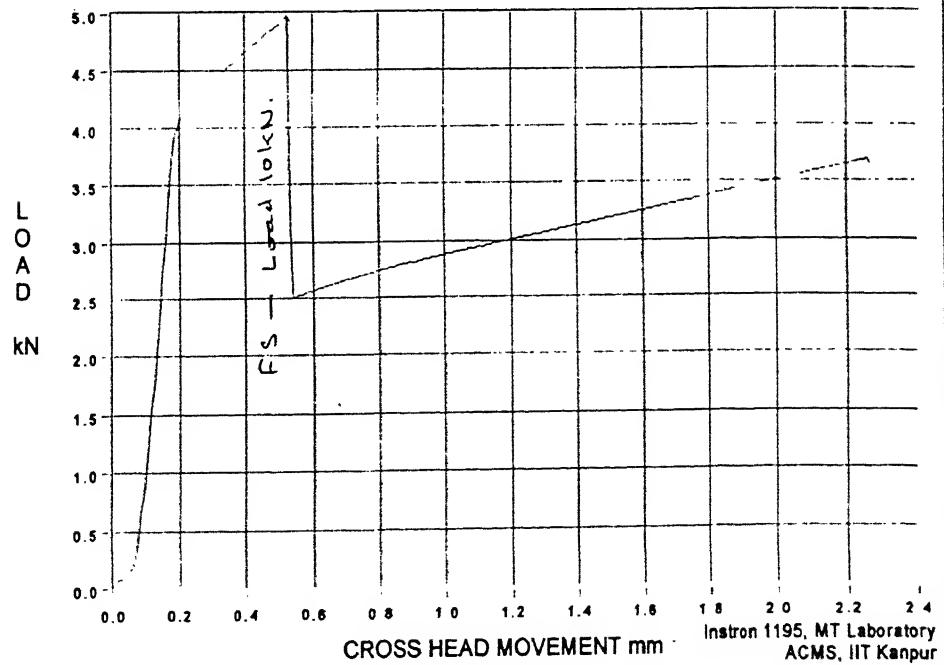
LOAD kN

Full Load (kN)

CROSS HEAD MOVEMENT mm

Instron 1195, MT Laboratory
ACMS, IIT Kanpur

compression of aluminium sample   03/09/98   14:47   q

Cross Section sq.mm	78.540
Gage Length mm	10.00
Crosshead mm/min	0.200
Full Scale kN	50.00
Scale Factor	1.000

LOAD kN vs CROSS HEAD MOVEMENT mm

Instron 1195, MT Laboratory
ACMS, IIT Kanpur

---

compression of aluminium sample   03/09/98   15:11
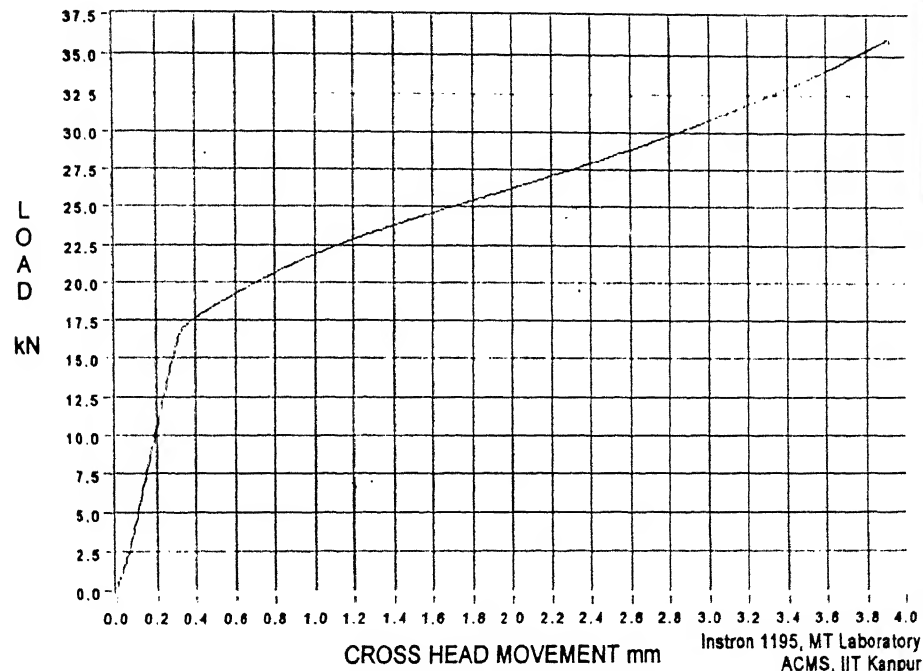
Cross Section sq.mm	113.097
Gage Length mm	12.00
Crosshead mm/min	0.500
Full Scale kN	50.00
Scale Factor	1.000

LOAD kN vs CROSS HEAD MOVEMENT mm

Instron 1195, MT Laboratory
ACMS, IIT Kanpur
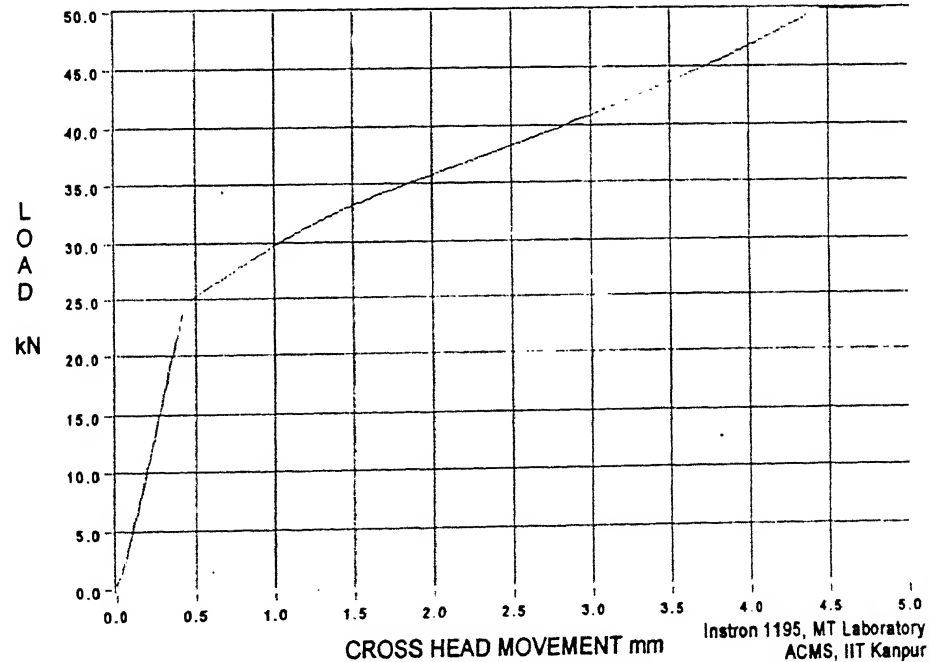
FILE C:\DATA\INSTRON\N090303.TXT

Cross Section sq.mm	283528
Gage Length mm	19.00
Crosshead mm/min	0.500
Full Scale kN	100.00
Scale Factor	1.000

LOAD kN

CROSS HEAD MOVEMENT mm

Instron 1195, MT Laboratory
ACMS, IIT Kanpur
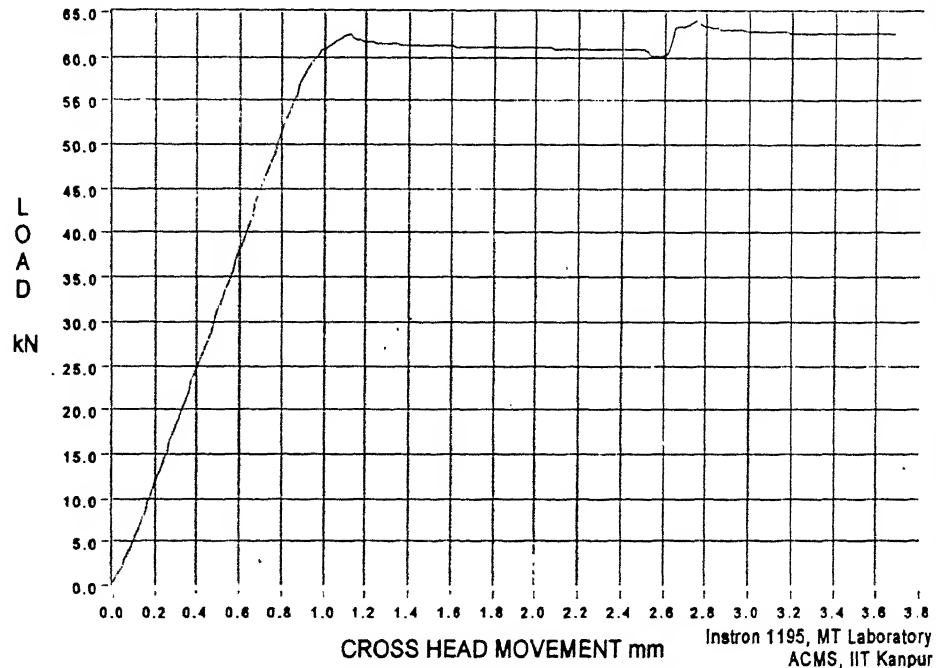
COMPRESSION TEST ON ALLUMINIUM 4   08/10/   t

FILE C:\DATA\INSTRON\N100806.TXT

Cross Section sq.mm	95.033
Gage Length mm	15.00
Crosshead mm/min	1.000
Full Scale kN	50.00
Scale Factor	1.000

LOAD kN

CROSS HEAD MOVEMENT mm

Instron 1195, MT Laboratory
ACMS, IIT Kanpur
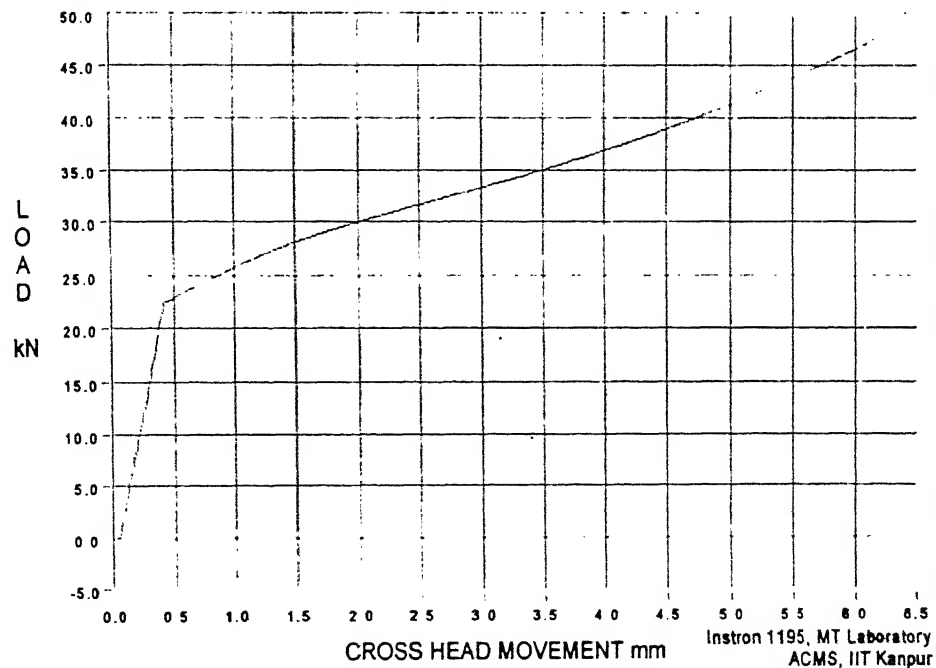
COMPRESSION TEST ON ALLUMINIUM 5   08/10/   U

Cross Section sq.mm	132.732
Gage Length mm	15.00
Crosshead mm/min	2.000
Full Scale kN	100.00
Scale Factor	1.000

CROSS HEAD MOVEMENT mm

Instron 1195, MT Laboratory
ACMS, IIT Kanpur
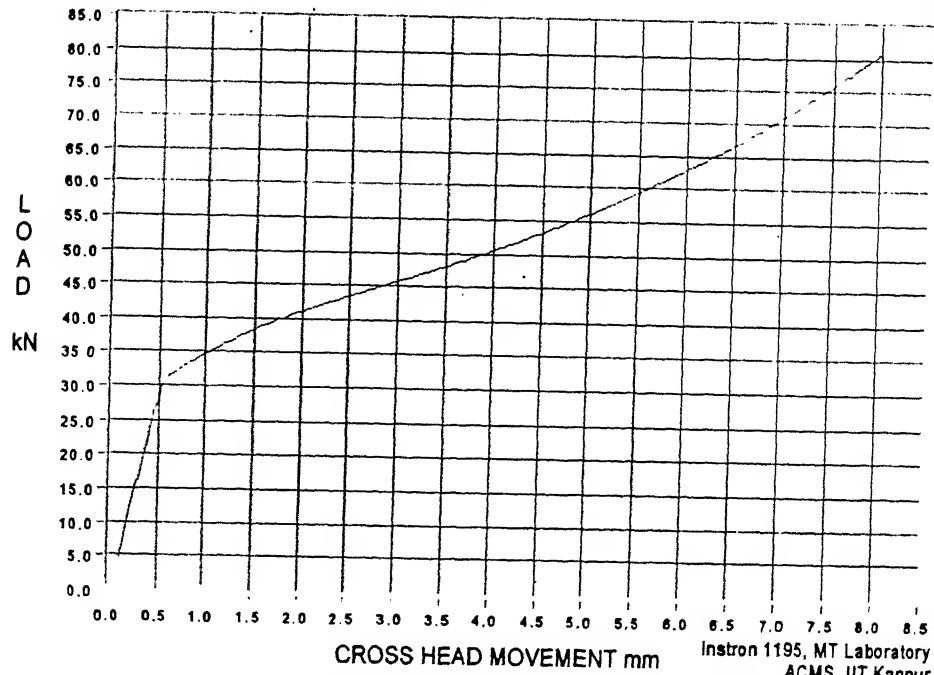
COMPRESSION TEST ON ALLUMINIUM 7   08/10/ 98   V

Cross Section sq.mm	176.715
Gage Length mm	22.00
Crosshead mm/min	5.000
Full Scale kN	100.00
Scale Factor	1.000

CROSS HEAD MOVEMENT mm

Instron 1195, MT Laboratory
ACMS, IIT Kanpur
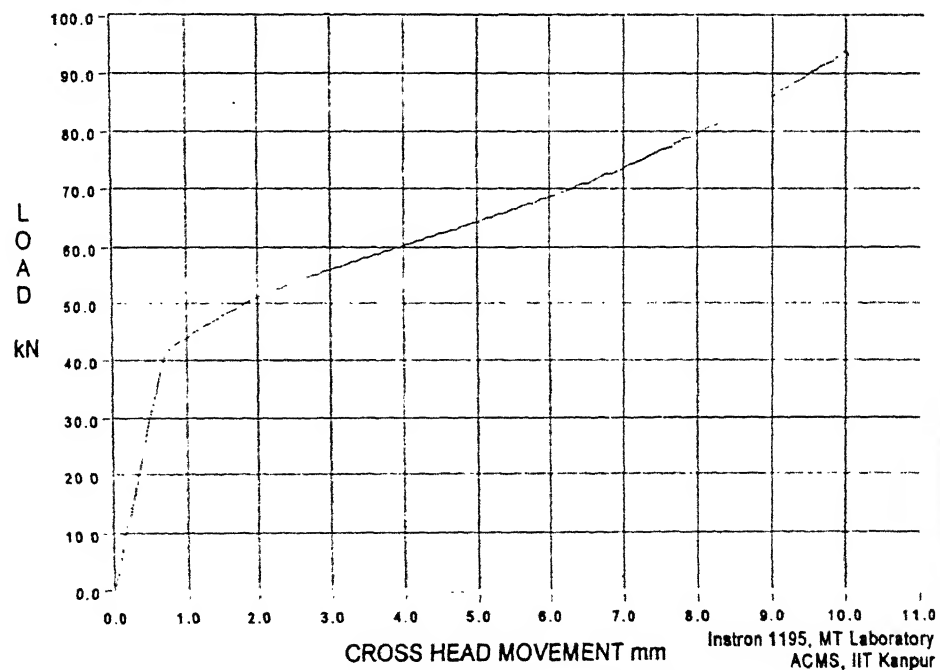
COMPRESSION TEST ON ALLUMINIUM 6   08/10/

W

Cross Section sq.mm	153.938
Gage Length mm	20.00
Crosshead mm/min	0.500
Full Scale kN	100.00
Scale Factor	1.000
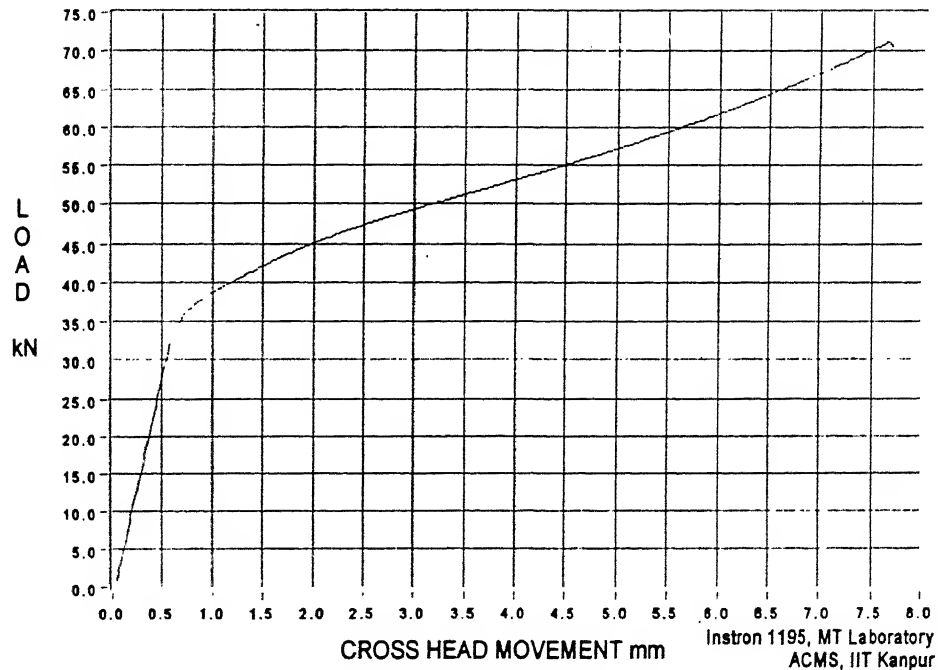
LOAD kN vs CROSS HEAD MOVEMENT mm

Instron 1195, MT Laboratory
ACMS, IIT Kanpur

Perms 1 0 5.00 0.00 0.00 9.20 04.00 1.00 0.65

Perms 2 04 $5.00E-3$ $9.00E-0$ $9.00E-0$ $0.00E+8$ $9.00E-0$ $0.00E-0$

X

COMPRESSION ON ALLUMINUM 1   08/10/98   15:48

FILE C:\DATA\INSTRON\IN100810.TXT

Cross Section sq.mm	
Gage Length mm	
Crosshead mm/min	
Full Scale kN	
Scale Factor	

LOAD kN vs CROSS HEAD MOVEMENT mm

Instron 1195, MT Laboratory
ACMS, IIT Kanpur
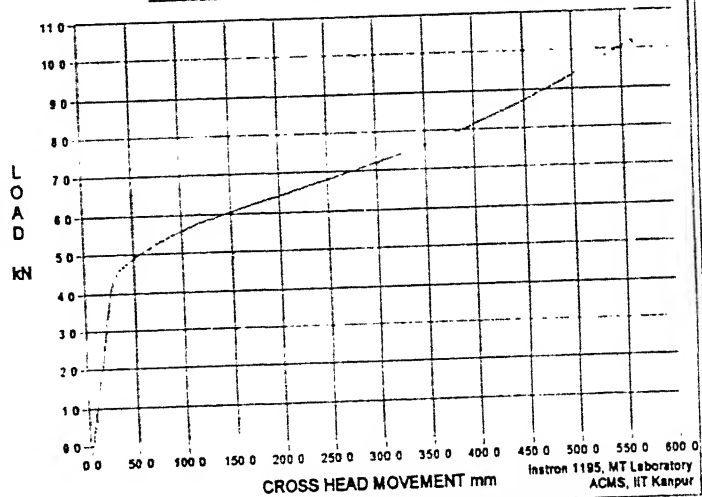
COMRESSION TEST OF ALUMINIUM 3   09/10/98

FILE ↳ C:\DATA\INSTRON\N100900.TXT

Cross Section sq.mm	63.617
Gage Length mm	10.00
Crosshead mm/min	0.100
Full Scale kN	100.00
Scale Factor	1.000

LOAD kN

CROSS HEAD MOVEMENT mm

Instron 1195, MT Laboratory
ACMS, IIT Kanpur
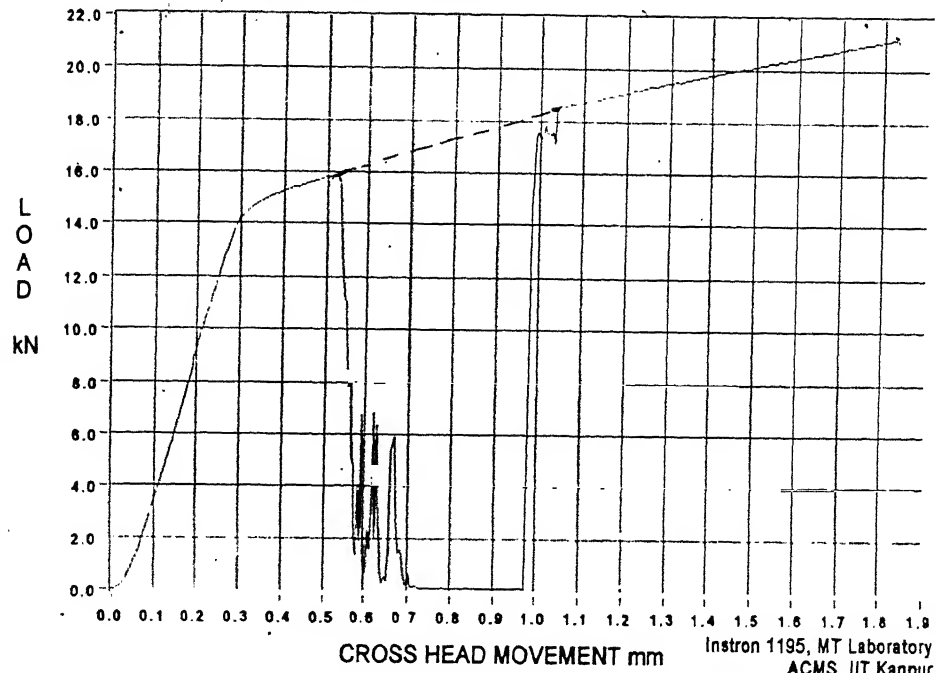
COMRESSION TEST OF ALUMINIUM 2   09/10/98

FILE ↳ C:\DATA\INSTRON\N100901.TXT

Cross Section sq.mm	38.485
Gage Length mm	10.00
Crosshead mm/min	0.050
Full Scale kN	50.00
Scale Factor	1.000

LOAD kN

CROSS HEAD MOVEMENT mm

Instron 1195, MT Laboratory
ACMS, IIT Kanpur